Atmos. Chem. Phys. Discuss., https://doi.org/10.5194/acp-2019-183
Manuscript under review for journal Atmos. Chem. Phys.
Discussion started: 22 May 2019

Atmospheric Chemistry and Physics Discussions

Development and application of observable response indicators for design of an effective ozone and fine particle pollution control strategy in China

Jia Xing[1,2], Dian Ding[1,2], Shuxiao Wang[1,2,*], Zhaoxin Dong[1,2], James T. Kelly[3], Carey Jang[3], Yun Zhu[4], Jiming Hao[1,2]

[1] State Key Joint Laboratory of Environmental Simulation and Pollution Control, School of Environment, Tsinghua University, Beijing 100084, China

[2] State Environmental Protection Key Laboratory of Sources and Control of Air Pollution Complex, Beijing 100084, China

[3] Office of Air Quality Planning and Standards, U.S. Environmental Protection Agency, Research Triangle Park, NC 27711, USA

[4] College of Environmental Science & Engineering, South China University of Technology, Guangzhou Higher Education Mega Center, Guangzhou, China

[*]Corresponding Author: Shuxiao Wang (email: shxwang@tsinghua.edu.cn; phone: +86-10-62771466; fax: +86-10-62773650)

Abstract

Designing effective control policies requires efficient quantification of the nonlinear response of air pollution to emissions. However, neither the current observable indicators nor the current indicators based on response-surface modeling (RSM) can fulfill this requirement. Therefore, this study developed new observable RSM-based indicators and applied them to ambient fine particulate matter ($PM_{2.5}$) and ozone (O_3) pollution control in China. The performance of these observable indicators in predicting O_3 and $PM_{2.5}$ chemistry was compared with that of the current RSM-based indicators. H_2O_2×HCHO/NO_2 and total ammonia ratio, which exhibited the best performance among indicators, were proposed as new observable O_3- and $PM_{2.5}$-chemistry indicators, respectively. Strong correlations between RSM-based and traditional observable indicators suggested that a combination of ambient concentrations of certain chemical species can serve as an indicator to approximately quantify the response of O_3 and $PM_{2.5}$ to changes in precursor

Atmos. Chem. Phys. Discuss., https://doi.org/10.5194/acp-2019-183
Manuscript under review for journal Atmos. Chem. Phys.
Discussion started: 22 May 2019

Atmospheric Chemistry and Physics Discussions

emissions. The observable RSM-based indicator for O_3 (observable peak ratio) effectively captured the strong NO_x-saturated regime in January and the NO_x-limited regime in July, as well as the strong NO_x-saturated regime in northern and eastern China and their key regions, including the Yangtze River Delta and Pearl River Delta. The observable RSM-based indicator for $PM_{2.5}$ (observable flex ratio) also captured strong NH_3-poor condition in January and NH_3-rich condition in April and July, as well as NH_3-rich in northern and eastern China and the Sichuan Basin. Moreover, analysis of these newly developed observable response indicators suggested that the simultaneous control of NH_3 and NO_x emissions produces greater benefits in provinces with higher $PM_{2.5}$ exposure by up to 12 μg m^{-3} $PM_{2.5}$ per 10 % NH_3 reduction compared with NO_x control only. Control of volatile organic compound (VOC) emissions by as much as 40 % of NO_x controls is necessary to obtain the co-benefits of reducing both O_3 and $PM_{2.5}$ exposure at the national level when controlling NOx emissions. However, the VOC-to-NOx ratio required to maintain benefits varies significantly from 0 to 1.2 in different provinces, suggesting that a more localized control strategy should be designed for each province.

Keywords: nonlinear response, precursor emissions, response surface model, ozone, $PM_{2.5}$, indicator

Atmos. Chem. Phys. Discuss., https://doi.org/10.5194/acp-2019-183
Manuscript under review for journal Atmos. Chem. Phys.
Discussion started: 22 May 2019

Atmospheric Chemistry and Physics Discussions

1. Introduction

Air pollution has attracted great attention because of its harmful effects on human health (Cohen et al., 2017), climate (Myhre et al., 2013), agriculture and ecosystems (Fuhrer et al., 2016), and visibility (Friedlander et al., 1977). In particular, ambient fine particulate matter ($PM_{2.5}$) and ozone (O_3) are among the top risk factors for global mortality (Forouzanfar et al., 2015; Cohen et al., 2017) and have increased the need to effectively control anthropogenic sources in order to reduce the ambient concentrations of $PM_{2.5}$ and O_3 (Wang et al., 2017). The challenge is that the dominant contributions to ambient $PM_{2.5}$ and O_3 arise from a series of chemical reactions among precursors, including sulfur dioxide (SO_2), nitrogen oxides (NO_x), ammonia (NH_3) and volatile organic compounds (VOCs) (Seinfeld et al., 2017). The complexity of the chemical reactions and pathways associated with variations in meteorological conditions and precursor levels results in strong nonlinear responses of $PM_{2.5}$ and O_3 to their precursor emission changes (West et al., 1999; Hakami et al., 2004; Cohan et la., 2005; Pun et al., 2007; Megaritis et al., 2013). Such nonlinearity issues are a major challenge for policy-makers to design an effective control strategy.

Chemical species in the atmosphere are often highly correlated with one another because of similarities in their atmospheric processes. Concentrations of secondary pollutants such as O_3 and $PM_{2.5}$ are typically determined based on the ambient levels of their precursors, implying that O_3 and $PM_{2.5}$ chemistry can be identified through a combination of concentrations of some of their related chemical species (i.e., indicators). The empirical kinetic modeling approach (EKMA) developed by the U.S. EPA quantifies the relationships of O_3 with its precursor concentrations based on O_3 chemistry (Freas et al., 1978; Gipson et al., 1981). The EKMA plot can aid inference of control strategy effectiveness (e.g., NO_x or VOC control) according to VOC-to-NO_x ratios. Several studies have developed "observable" indicators by relating O_3 to reactive nitrogen concentrations and species related to atmospheric oxidation. Such

indicators include NO_y, H_2O_2/HNO_3, $HCHO/NO_2$ and $H_2O_2/(O_3+NO_2)$ (Milford et al., 1994; Sillman, 1995; Tonnesen and Dennis, 2000; Sillman and He, 2002), which can be used to identify NOx-saturated or -limited regimes. Regarding $PM_{2.5}$ chemistry (more specifically for inorganic $PM_{2.5}$ sensitivities to NH_3 and NO_x), indicators such as the degree of sulfate neutralization (DSN), gas ratio (GR), and adjusted gas ratio (AdjGR) have been developed to identify NH_3-poor or -rich conditions (Ansari and Pandis, 1998; Takahama et al., 2004; Pinder et al., 2008; Dennis et al., 2008). These indicators can be derived from surface-monitoring observations (Peng et al., 2006), modeling simulations (Wang et al., 2010), or even satellite retrievals (Jin et al., 2017; Sun et al., 2018), and then examined using three-dimensional chemical transport models (CTMs) (Jiménez et al., 2004; Zhang et al., 2009; Liu et al., 2010; Ye et al., 2016). The indicator-based method can be efficient in determining the chemical regime in the current scenarios and in qualitatively estimating O_3 and $PM_{2.5}$ sensitivities to small perturbations in precursor emissions or ambient concentrations without involving complex CTMs. However, traditional indicator methods are unable to quantify the extent of the chemistry regime (Pinder et al., 2008); hence, the traditional observable indicators provide policy-makers limited information for reducing O_3 and $PM_{2.5}$ pollution.

The sensitivity of O_3 and $PM_{2.5}$ to precursor emissions can be explored by running multiple brute-force CTM simulations. For instance, the response surface model (RSM) developed from brute-force simulations can generate a wide range of O_3 and $PM_{2.5}$ responses to precursor emissions ranging from fully controlled to doubled emissions (i.e., -100 % to 100 % change relative to the baseline emission) (Xing et al., 2011; Wang et al., 2011). Based on the RSM, the chemical response indicators of Peak Ratio (PR) and Flex Ratio (FR) have been designed to identify regimes of O_3 and $PM_{2.5}$ chemistry, respectively. In contrast to the observable indicators, the PR and FR are meaningful values that represent the exact transition point at which a chemistry regime converts to another regime. With the recent development of the polynomial function-based RSM (pf-RSM), the PR and FR can be easily calculated (Xing et al., 2018).

89 However, this method is built on at least 20 CTM simulations; in other words, the estimating the PR and
90 FR requires considerable computing resources. As a result, RSM use remains limited despite recent
91 improvements in RSM efficiency (Xing et al., 2017).

92 Over the preceding decade, China's air quality has undergone substantial changes. In particular, the
93 enactment of the *Air Pollution Prevention and Control Action Plan* from 2013 to 2017 greatly reduced
94 $PM_{2.5}$ exposure (Zhao et al., 2018; Ding et al., 2019a). However, during this period, significant increases
95 in O_3 concentrations were observed in most Chinese cities (Li et al., 2018). The rate of increase in O_3
96 concentration (based on the 90th percentile of daily maximum of 8-hr running average) was approximately
97 27 %, 19 %, and 8 % in the North China Plain (NCP), Yangtze River Delta (YRD), and Pearl River Delta
98 (PRD), respectively (Ding et al., 2019b). Greater control over anthropogenic sources must be enforced to
99 reduce $PM_{2.5}$ and O_3 concentrations (Lu et al., 2018). Notably, accurate quantification of the nonlinear
100 responses of O_3 and $PM_{2.5}$ to their precursor emissions is critical and a prerequisite for effective mitigation
101 of severe pollution in China.

102 Indicator studies have demonstrated that the nonlinear response of O_3 and $PM_{2.5}$ to precursors can
103 be estimated by using ambient concentrations of related chemical species. It is expected that the response
104 indicators originally derived from RSM predictions (i.e., PR and FR) can also be calculated using a
105 combination of ambient concentrations of certain chemical species, enabling these indicators to become
106 "observable" indicators rather than being dependent on numerous CTM simulations. Above all, the design
107 of an effective O_3 and $PM_{2.5}$ control strategy requires efficient quantification of air pollutant sensitivity to
108 precursor emissions. To support the needs of policy design for O_3 and $PM_{2.5}$ control, this study developed
109 effective indicators that not only represent O_3 and $PM_{2.5}$ chemistry but also aid in determining the most
110 feasible emission reduction path, similar to the benefits provided by RSM-based indicators. The flow of
111 this study is presented in Fig. 1. The new observable response indicators were developed by investigating

112 the link between observable and RSM-based indicators in China.

113 The remainder of this paper is structured as follows: Section 2 presents the detailed methods for
114 CTM modeling, RSM configuration and response indicator development. Section 3 presents the
115 evaluation of the performance of observable indicators in predicting the chemistry regime and the
116 development of the observable response indicators and discusses their policy implications. Section 4
117 summarizes the main conclusions of this study.

118 2. Method

119 2.1. Configuration of the CTM and RSM

120 In this study, the Community Multi-scale Air Quality (CMAQ) model (version 5.2) was used to
121 simulate the baseline concentrations of O_3 and $PM_{2.5}$ and their responses in numerous emission control
122 scenarios with different emission change ratios. The simulation was conducted on a domain covering
123 China with 27 km × 27 km horizontal resolution (Fig. 2). In 2017, January, April, July, and October were
124 simulated to represent winter, spring, summer, and fall, respectively. An annual level was estimated as the
125 average of the levels in these four months. The concentration data was analyzed based on the monthly
126 average for afternoon O_3 (12:00–18:00 China Standard Time when O_3 was the highest across a day), and
127 monthly average for 24-h $PM_{2.5}$. To approximate exposure concentrations, we also estimated population-
128 weighted O_3 and $PM_{2.5}$ at the regional or national level by averaging the gridded concentrations weighted
129 by the population in each grid cell. The gridded population data were obtained from the 1 km × 1 km
130 LandScan population dataset in 2016 (Oak Ridge National Laboratory, 2013).

131 The anthropogenic emission data were developed by Tsinghua University by using a bottom-up
132 method (Ding et al., 2019a), with updated activity data from the 2017 China statistical yearbook as well
133 as the latest application rates of end-of-pipe control technologies based on the governmental bulletin and
134 reports. The anthropogenic emissions were gridded into 27 km × 27 km horizontal resolution to match the

Atmos. Chem. Phys. Discuss., https://doi.org/10.5194/acp-2019-183
Manuscript under review for journal Atmos. Chem. Phys.
Discussion started: 22 May 2019

CMAQ model (Fig. S1). The 2017 biogenic emissions over China were generated using the Model for Emissions of Gases and Aerosols from Nature (MEGAN; version 2.04). The meteorology field, driven by the Weather Research and Forecasting Model (WRF; version 3.7), followed the same configuration as that in our previous study (Ding et al., 2019a,b), and thus included the Morrison double-moment microphysics scheme, the RRTMG radiation scheme, Kain-Fritsch cumulus cloud parameterization, the Pleim-Xiu land-surface physics scheme, and the ACM2 PBL physics scheme. We used NCEP FNL (Final) Operational Global Analysis data for the initial and boundary conditions in the WRF. The comparison with observation data from the National Climatic Data Center suggested agreeable performance of the WRF model for simulating wind speed, humidity and temperature (Table S1). The CMAQ model performance in reproducing O_3 and $PM_{2.5}$ concentrations was evaluated by comparison with the ground-based observations (Fig. S2), which suggested acceptable CMAQ model performance that met the recommended benchmark (Ding et al., 2019a,b).

The RSM was developed based on multiple CTM simulations for various emission-control scenarios according to the brute-force method. Identical to our previous RSM studies (Xing et al., 2017, 2018), the responses of O_3 and $PM_{2.5}$ to precursor emissions were analyzed using the baseline case and 40 control scenarios using the Latin Hypercube Sample method for four control variables, namely the emission ratios of NO_x, SO_2, NH_3, and VOCs. The control matrix is provided in Table S2. The performance of the RSM system has been thoroughly examined in our previous studies (Zhao et al., 2017; Xing et al., 2018; Ding et al., 2019b).

2.2. RSM-based indicators of O_3 and $PM_{2.5}$ chemistry

Based on the developed pf-RSM, the nonlinear responses of O_3 and $PM_{2.5}$ concentrations to precursor emissions can be represented as follows:

$$\Delta Conc = \sum_{i=1}^{n} X_i \cdot (\Delta E_{NOx})^{a_i} \cdot (\Delta E_{SO2})^{b_i} \cdot (\Delta E_{NH3})^{c_i} \cdot (\Delta E_{VOCs})^{d_i} \quad (1)$$

Atmos. Chem. Phys. Discuss., https://doi.org/10.5194/acp-2019-183
Manuscript under review for journal Atmos. Chem. Phys.
Discussion started: 22 May 2019

Atmospheric Chemistry and Physics Discussions

where $\Delta Conc$ is the change in O_3 or $PM_{2.5}$ concentration from the baseline concentration calculated from a polynomial function of four variables (ΔE_{NOx}, ΔE_{SO2}, ΔE_{NH3}, ΔE_{VOCs}); ΔE_{NOx}, ΔE_{SO2}, ΔE_{NH3}, and ΔE_{VOCs} are the change ratios of NO_x, SO_2, NH_3, and VOC emissions (i.e., *ΔEmissions / Baseline_Emissions*), respectively, relative to the baseline emissions (baseline = 0); and a_i, b_i, c_i, and d_i are the nonnegative integer powers of ΔE_{NOx}, ΔE_{SO2}, ΔE_{NH3}, and ΔE_{VOCs}, respectively. X_i is the coefficient of term i for the 14 (n) terms listed in Table 1.

The terms used to represent $PM_{2.5}$ and O_3 responses were determined in designing the pf-RSM (Table 1). The high-degree terms of NO_x, VOCs and NH_3 represent their strong nonlinear contributions to O_3 or $PM_{2.5}$. The interaction terms of NO_x and VOC for $PM_{2.5}$ and O_3 represent the nonlinearity in atmospheric oxidations, whereas those of NO_x and NH_3 for $PM_{2.5}$ represent aerosol thermodynamics (Xing et al., 2018).

X_i was fitted by 40 CTM control scenarios for each spatial grid cell. The X_i values in the pf-RSM for annual-averaged population-weighted O_3 and $PM_{2.5}$ concentrations in 31 provinces in China are provided in Table S3 and Table S4, respectively. The terms with first degree for NOx, SO_2, NH_3, and VOCs represent the first derivative of $PM_{2.5}$ and O_3 response to each precursor emission. O_3 was more sensitive to NO_x (term X_5) and VOCs (term X_6) than to SO_2 (term X_{13}) or NH_3 (term X_{14}), and O_3 sensitivity was negative to NO_x but positive to VOCs in most provinces. $PM_{2.5}$ sensitivities to the four precursors (terms X_1, X_2, X_5 and X_{11} for VOCs, NH_3, SO_2, and NO_x, respectively) were comparable, whereas $PM_{2.5}$ sensitivity to NO_x could be negative or positive.

The nonlinearities of O_3 and $PM_{2.5}$ to precursors were mainly determined by high-order and interaction terms. To illustrate such nonlinearities further, we used a series of isopleths, as shown in Fig. 3, as an example to present the national-averaged $PM_{2.5}$ response to SO_2 and NH_3, as well as $PM_{2.5}$ and O_3 responses to NO_x and VOCs in different months. Strong nonlinearity was noted in $PM_{2.5}$ sensitivity to

Atmos. Chem. Phys. Discuss., https://doi.org/10.5194/acp-2019-183
Manuscript under review for journal Atmos. Chem. Phys.
Discussion started: 22 May 2019

Atmospheric Chemistry and Physics Discussions

181 NH_3, and in O_3 and $PM_{2.5}$ sensitivities to NO_x. $PM_{2.5}$ sensitivity to NH_3 increased alongside the transition
182 of $PM_{2.5}$ chemistry from the NH_3-rich condition (typically at high NH_3 emission ratios) to the NH_3-poor
183 condition (typically at low NH_3 emission ratios). O_3 and $PM_{2.5}$ sensitivities to NO_x were negative under
184 the NO_x-saturated regime (typically at high NO_x emission ratios) but became positive under the NO_x-
185 limited regime (typically at low NO_x emission ratios). In addition, the transition points (corresponding to
186 the NO_x or NH_3 ratios at which the chemical regime for O_3 or $PM_{2.5}$ chemistry changed) varied by time
187 (Fig. 3) and space (see the isopleths at different provinces in Figs S3-S6). In general, the NH_3-poor
188 condition appears in winter because of low NH_3 evaporation and little agriculture activity which is a
189 dominant NH_3 source. The strong NO_x-saturated condition appears in winter when photolysis is less active
190 than in other seasons, and concentrates in industrial regions with abundant NO_x emissions.

191 To further quantify the aforementioned nonlinearity, two RSM-based response indicators (i.e., the
192 PR for O_3 and FR for $PM_{2.5}$) were calculated as described in our previous studies (Xing et al., 2011, 2018;
193 Wang et al., 2011).

194 For O_3, the PR can be directly calculated as follows:

195 $$PR = 1 + \Delta E_{NOx}|_{\frac{\partial \Delta Conc_{O3}}{\partial \Delta E_{NOx}}=0} \quad E_{NOx} \epsilon [a, b] , \qquad (2)$$

196 where $\frac{\partial \Delta Conc_{O3}}{\partial \Delta E_{NOx}}$ is the first derivative of the $\Delta Conc_{O3}$ to ΔE_{NOx}, which can be derived as follows:

197 $$5 * X_1 * \Delta E_{NOx}{}^4 + 4 * X_2 * \Delta E_{NOx}{}^3 + 3 * X_3 * \Delta E_{NOx}{}^2 + 2 * X_4 * \Delta E_{NOx} + X_5 = 0 \quad (3)$$

198 The PR is the NO_x emissions (represented as $1 + \Delta E_{NOx}$) that produce maximum O_3 concentration
199 under the baseline VOC emissions. For PR < 1, the baseline condition is NO_x saturated, and the level of
200 simultaneous control of VOCs to prevent an increase in O_3 levels from the NO_x controls must be
201 understood. This level is defined by the ratio of VOCs to NO_x corresponding to the PR (i.e., VNr) and is
202 calculated as follows:

Atmos. Chem. Phys. Discuss., https://doi.org/10.5194/acp-2019-183
Manuscript under review for journal Atmos. Chem. Phys.
Discussion started: 22 May 2019

Atmospheric Chemistry and Physics Discussions

$$VNr = r|_{\frac{\partial \Delta Conc_{O3}}{\partial \Delta E_{NOx}}=0} \quad when\ PR < 1 \quad , r = {\Delta E_{VOC}}/{\Delta E_{NOx}}, \quad (4)$$

where $\frac{\partial \Delta Conc_{O3}}{\partial \Delta E_{NOx}}$ is the first derivative of the $\Delta Conc_{O3}$ to ΔE_{NOx} when $\Delta E_{VOC} = r \times \Delta E_{NOx}$; the VNr can be calculated using the following equation:

$$VNr = -\frac{X_5}{X_6} \quad (5)$$

For $PM_{2.5}$, the FR can be directly calculated from the polynomial function of $PM_{2.5}$ by estimating the second derivative of the $PM_{2.5}$ response to NH_3 emissions without considering interaction with other pollutants (Xing et al., 2018). In this study, we selected a simplified method to calculate the FR, estimated as the corresponding NH_3 emission ratio when the $PM_{2.5}$ sensitivity to NH_3 and NO_x emissions is equal under the baseline conditions (similar to the definition in Wang et al (2011), but here we calculated the sensitivity of $PM_{2.5}$ instead of nitrate in this study):

$$FR = 1 + \Delta E_{NH3}|_{\frac{\partial \Delta Conc_{PM}}{\partial \Delta E_{NH3}}=\frac{\partial \Delta Conc_{PM}}{\partial \Delta E_{NOx}}} \quad \Delta E_{NH3} \epsilon [a, b], \Delta E_{NOx} = 0, \quad (6)$$

where $\frac{\partial \Delta Conc_{PM}}{\partial \Delta E_{NH3}}$ and $\frac{\partial \Delta Conc_{PM}}{\partial \Delta E_{NOx}}$ are the first derivatives of the $\Delta Conc_{PM}$ to ΔE_{NH3} and ΔE_{NOx}, respectively, and ΔE_{NH3} can be obtained as follows:

$$3 * X_4 * {\Delta E_{NH3}}^2 + (2 * X_3 - X_{10}) * \Delta E_{NH3} + X_2 - X_{11} = 0 \quad (7)$$

The FR is the NH_3 emissions (represented as $1 + \Delta E_{NH3}$) that correspond to the inflection point between NH_3-rich and -poor conditions under baseline NOx emissions. A FR greater than 1 indicates that the baseline condition is NH_3 poor, and a FR less than 1 indicates that the baseline condition is NH_3 rich. The extra benefit in $PM_{2.5}$ reduction (denoted as ΔC_NH_3) from simultaneous NH_3 controls in the same percentage as the required NO_x controls can be quantified as follows:

$$\Delta C\_NH_3 = \left(\frac{\partial \Delta Conc_{PM2.5}}{\partial \Delta E_{NOx}}|_{\Delta E_{NH3}=\Delta E_{NOx}}\right) - \left(\frac{\partial \Delta Conc_{PM2.5}}{\partial \Delta E_{NOx}}|_{\Delta E_{NH3}=0}\right), \quad (8)$$

where

Atmos. Chem. Phys. Discuss., https://doi.org/10.5194/acp-2019-183
Manuscript under review for journal Atmos. Chem. Phys.
Discussion started: 22 May 2019

Atmospheric Chemistry and Physics Discussions

224 $\frac{\partial \Delta Conc_{PM2.5}}{\partial \Delta E_{NOx}}|_{\Delta E_{NH3}=\Delta E_{NOx}}$ is the first derivative of the $\Delta Conc_{PM2.5}$ response to ΔE_{NOx} when $\Delta E_{NH3} =$

225 ΔE_{NOx}, and

226 $\frac{\partial \Delta Conc_{PM2.5}}{\partial E_{NOx}}|_{E_{NH3}=0}$ is the first derivative of the $\Delta Conc_{PM2.5}$ response to ΔE_{NOx} when $\Delta E_{NH3} = 0$.

227 ΔC_NH_3 can be calculated as follows:

228 $$\Delta C\_NH_3 = X_2 \qquad (9)$$

229 **2.3. Observable indicators of O_3 and $PM_{2.5}$ chemistry**

230 Zhang et al. (2009) summarized the various observable indicators with their corresponding transition
231 values to identify O_3 and $PM_{2.5}$ chemistry: O_3 indicators were H_2O_2/HNO_3, $H_2O_2/(O_3+NO_2)$, NO_y, O_3/NO_x,
232 O_3/NO_y, O_3/NO_z, $HCHO/NO_y$, and $HCHO/NO_2$, and the $PM_{2.5}$ indicators were the DSN, GR, and AdjGR
233 (defined in Text S1); these indicators have been used extensively in previous research (Liu et al., 2010;
234 Wang et al., 2011; Ye et al., 2016). In the current study, we evaluated all the aforementioned indicators
235 except DSN (DSN is included in the definition of the AdjGR, thus it was not considered as a separate
236 indicator in this study). The orignal transition values, summarized by Zhang et al (2009), are listed in
237 Table 2. In the present study, we examined these transition values and compared their performance in
238 predicting O_3 and $PM_{2.5}$ chemistry. Because the RSM-based indicators, PR and FR, are calculated using
239 the multiple CTM simulations that use state-of-the-science representations of O_3 and $PM_{2.5}$ chemistry,
240 these indicators were assumed to represent the true condition for comparison with the condition predicted
241 using observable indicators. The performance of each observable indicator is described by its success rate,
242 which is the ratio of the number of correct predictions to the total number of predictions. A correct
243 prediction is indicated by the observable indicator providing consistent results for O_3 or $PM_{2.5}$ chemistry
244 as suggsted by PR or FR. The comparison is only conducted for spatial grid cells with valid PR or FR
245 values within the range of 0 (fully controlled emissions) to 2 (double emissions).

Atmos. Chem. Phys. Discuss., https://doi.org/10.5194/acp-2019-183
Manuscript under review for journal Atmos. Chem. Phys.
Discussion started: 22 May 2019

Atmospheric Chemistry and Physics Discussions

246 As RSM-based indicators, the PR and FR have meaningful values that can be used to illustrate the
247 extent of the chemistry regime. The linkage of observable indicators with the PR and FR was investigated
248 by performing a linear-log regression of the value of the original observable indicator and the values of
249 the PR or FR as follows:

250 $$log(Y) = A \cdot X + B \quad (10)$$

251 where Y is an observable indicator for O_3 or $PM_{2.5}$, X is the RSM-based indicator (i.e., PR for O_3 or FR
252 for $PM_{2.5}$), and the coefficients A and B are estimated based on statistical regression. Therefore, the
253 observable response indicators (X') can be calculated as follows:

254 $$X' = \frac{log(Y) - B}{A} \quad (11)$$

255 The observable response indicators have the same policy implication as that of PR or FR, but they
256 can be directly calculated from the baseline concentrations of certain chemical species rather than being
257 derived from multiple CTM simulations. Therefore, these indicators are considerably more efficient than
258 are traditional RSM-based indicators.

259 # 3. Results

260 ## 3.1. Evaluating observable indicator performance in predicting chemistry regimes

261 ### 3.1.1. O_3

262 Observable indicators and the PR are compared in Fig. 4, and the performance of observable
263 indicators in predicting O_3 chemistry is summarized in Table 2. In general, strong correlation was noted
264 between the observable indicators and PR. The indicator with the highest annual success rate was
265 H_2O_2/HNO_3 approximately 73.4 %, with a value of 0.2 for the transition from NO_x-saturated to NO_x-
266 limited conditions. However, the original transition value of 0.2 for H_2O_2/HNO_3 tended to be too low,
267 particularly in April, July, and October (see Fig. 4a). This study found that the annual success rate of

H_2O_2/HNO_3 could be increased to 80.5 % if 0.3 was used as the transition value. This finding was consistent with corresponding findings in previous studies, which have suggested the transition values of H_2O_2/HNO_3 within the range of 0.2-3.6 at different locations and in different seasons (Sillman, 1995; Sillman et al, 1997; Lu and Chang, 1998; Tonnesen and Dennis, 2000; Hammer et al, 2002; Liang et al, 2006; Zhang et al., 2009). $H_2O_2/(O_3+NO_2)$, with a transition value of 0.02, also exhibited a high annual success rate of 66.4 %; this rate could be increased to 71.1 % by applying a transition value of 0.005 because the original transition value was too high, particularly in January, April, and October (see Fig. 4b). $HCHO/NO_y$ and $HCHO/NO_2$ exhibited relatively low performance, particularly in April and July, because the original transition values appeared to be too high (Fig. 4h and i). However, the performance of $HCHO/NO_y$ and $HCHO/NO_2$ could be greatly improved by using lower transition values, with increased annual success rates as high as 76 %. The transition values of the indicators NO_y, O_3/NO_x, O_3/NO_y, and O_3/NO_z were suitable for estimating annual levels if only one unique transition value was applied for all months (apparently, these transition values for O_3/NO_x, O_3/NO_y and O_3/NO_z in January, and NO_x in April and July may have been too low). However, their success rates (all < 70 %) were not as high as those of other indicators. The inferior performance of the three O_3-involved indicators (O_3/NO_x, O_3/NO_y and O_3/NO_z) may have been associated with the considerable effects of background O_3, which cannot be removed easily.

Because $H_2O_2/(O_3+NO_2)$ and $HCHO/NO_2$ exhibited good performance in predicting O_3 chemistry, this study proposed a new indicator combining these two indicators, namely $H_2O_2 \times HCHO/NO_2$, with a transition value of 0.3. The results suggested that this new indicator has the highest annual success rate, namely 87.3 %, among all the indicators. Studies (Sillman, 1995; Tonnesen and Dennis, 2000) have suggested that HCHO is approximately proportional to the VOC reactivity (i.e., the weighted sum of the reactions of VOCs with OH) and that $HCHO/NO_2$ closely approximates the competition between OH

Atmos. Chem. Phys. Discuss., https://doi.org/10.5194/acp-2019-183
Manuscript under review for journal Atmos. Chem. Phys.
Discussion started: 22 May 2019

Atmospheric Chemistry and Physics Discussions

reactions with VOC and NO_2 that is central to O_3 chemistry. H_2O_2 derives from a key radical termination pathway under low NO_x conditions ($HO_2 + HO_2 \rightarrow H_2O_2 + O_2$). Comparison of H_2O_2 with NO_y or HNO_3, which derives from a key radical termination pathway under high NO_x conditions, $OH + NO_2 \rightarrow HNO_3$) represents the relative abundance of VOCs to NO_x. The new hybrid indicator incorporates information from the two individual indicators and could potentially be more robust.

3.1.2 $PM_{2.5}$

We selected the GR and AdjGR as observable indicators for $PM_{2.5}$ chemistry to identify NH_3-poor or NH_3-rich conditions. Comparison of GR and AdjGR with the FR is detailed in Fig. 5. AdjGR performance was much higher than that of the GR, with a larger annual success rate of 74.1 % compared with the GR's 55.6 % (see Table 3). The transition value of the GR appeared to be too low in all months (Fig. 5a). This result was consistent with those of previous studies; the AdjGR tends to be a more robust indicator because in contrast to the GR, it does not require an assumption of full sulfate neutralization (Zhang et al., 2009). The improvement of AdjGR compared to GR is the greatest in January and the smallest in July (Table 3). This is consistent with Pinder et al. (2008) who showed that accounting for DSN is important under cold temperatures but GR and AdjGR converge for higher temperatures.

This study designed a new indicator, total ammonia ratio (TAR), where the sulfate concentration is involved in the calculation, as follows:

$$TAR = \frac{[TA]^2}{[TN]\times[TS]} = \frac{[NH_3]\times[NH_4^+]}{([HNO_3]+[NO_3^-])\times[SO_4^{2-}]}, \qquad (12)$$

where $[TN]$ and $[TS]$ are the total molar concentrations of nitrate ($[HNO_3] + [NO_3^-]$) and sulfate ($[SO_4^{2-}]$), respectively, and TAR is the relative abundance of total ammonia to nitrate and sulfate, regarded as the product of $[TA]/[TN]$ and $[TA]/[TS]$. To simplify the calculation, $[TA]^2$ is assumed to be the product of the molar concentration of ammonia gas $[NH_3]$ and ammonium $[NH_4^+]$.

Atmos. Chem. Phys. Discuss., https://doi.org/10.5194/acp-2019-183
Manuscript under review for journal Atmos. Chem. Phys.
Discussion started: 22 May 2019

The performance of TAR in predicting $PM_{2.5}$ chemistry was slightly higher than that of AdjGR, as demonstrated by the higher success rate of TAR than that of AdjGR in all months. The annual success rate of TAR was 79.6 %, with a transition value of 10 (Table 3).

3.2 Developing the observable responsive indicators

3.2.1 O_3

Fig. 6 presents the log-linear regressions of the O_3 observable indicators on the PR indicator derived from the RSM. In general, all observable indicators exhibited strong correlations with the PR (all except NO_y presented positive correlations with the PR), with varying R^2 values (0.08 – 0.75). The indicators including NO_y, O_3/NO_x, O_3/NO_y, and O_3/NO_z, which had relatively low success rates, exhibited weaker correlation with the PR ($R^2 < 0.31$; Fig. 6c-f). The newly developed $H_2O_2 \times HCHO/NO_2$ indicator exhibited the strongest correlation with the PR ($R^2 = 0.75$), implying that the log-linear combination of the H_2O_2, HCHO, and NO_2 baseline concentrations could approximate the responsive PR indicator to quantify O_3 chemistry. Other indicators can also be used to approximately estimate the PR based on the regression coefficients shown in Fig. 6; however, their correlations with the PR were not as strong as those with $H_2O_2 \times HCHO/NO_2$.

To evaluate the ability of the observable PR (oPR; estimated based on $H_2O_2 \times HCHO/NO_2$) to represent the spatial and temporal variation of O_3 chemistry, the spatial distribution of the PR and oPR in the four study months was compared across the simulated domain (Fig. 7). The oPR successfully captured the strong NO_x-saturated regime in January (PR < 1) and the NO_x-limited (PR > 1) regime in July.

In addition, the PR and oPR suggested a consistently strong NO_x-saturated regime in northern and eastern China and key regions such as the YRD and PRD. The domain-averaged oPRs were 0.97, 1.52, 1.73, and 1.37 in January, April, July, and October, respectively; these values are similar to the PRs (0.77, 1.24, 1.38, and 1.17, respectively). Thus, the oPR may approximate the PR to quantify the O_3 chemistry,

336 even on a large spatial and temporal scale.

337 **3.2.2. $PM_{2.5}$**

338 The correlations between $PM_{2.5}$ observable indicators and the responsive FR indicator derived from
339 the RSM were investigated (Fig. 8). The AdjGR has the lowest R^2 (0.40) because of its high variations for
340 the NH_3-poor condition (Fig. 5b). A stronger positive correlation was noted between the GR and FR (R^2
341 = 0.57); however, the success rate of the GR was the lowest among all the indicators (the success rate of
342 the GR increased when the transition value was set as the median value of the GR, namely 5, at an FR of
343 1). The TAR exhibited the strongest positive correlation with the FR (R^2 = 0.60), implying that the FR can
344 be approximately estimated by the log-linear combination of baseline concentrations of ammonia gas,
345 nitric acid gas, particulate ammonium, sulfate, and nitrate.

346 The capability of the observable FR (oFR; estimated based on the TAR indicator) in representing
347 the spatial and temporal variation of $PM_{2.5}$ chemistry is illustrated in Fig. 9. Both the FR and oFR
348 suggested strong NH_3-poor condition (FR > 1)in January and NH_3-rich condition (FR < 1) in April and
349 July. The oFR suggested strong NH_3-rich condition in northern and eastern China and the Sichuan Basin;
350 these findings were consistent with those for the FR. The domain-averaged oFRs were 1.56, 1.05, 0.86,
351 and 1.24 in January, April, July, and October, respectively, with the strongest NH_3-poor condition in
352 January and NH_3-rich condition in July. These findings were comparable with the FRs of 1.47, 1.16, 0.95,
353 and 1.19 for the four study months, respectively, suggesting that the oFR can approximate the FR to
354 quantify the $PM_{2.5}$ chemistry and its spatial and temporal variations.

355 **3.3. Policy implications**

356 **3.3.1. O_3**

357 The responsive PR indicator may help policy-makers to understand the status and extent of O_3

Atmos. Chem. Phys. Discuss., https://doi.org/10.5194/acp-2019-183
Manuscript under review for journal Atmos. Chem. Phys.
Discussion started: 22 May 2019

chemistry in the current scenarios. A lower PR (< 1) suggested a NO_x-saturated regime. Moreover, the VNr could be used to inform policy-makers about the level of simultaneous control of VOCs required to prevent an increase in O_3 levels from NO_x controls. In general, the VNr is negatively correlated with the PR because a lower PR implies a stronger NO_x-saturated regime, which in turn requires more simultaneous VOC control with NO_x. By contrast, a higher PR implies a weaker NO_x-saturated or even NO_x-limited regime, which requires less or no simultaneous control of VOCs with NO_x. The negative correlation between VNr and the PR was quantified by the simple linear regression of VNr on PR (Fig. S7). A high R^2 (approximately 0.82) suggested that the VNr originally derived from the RSM can also be approximately estimated from the PR or oPR.

Figure 10 presents a comparison of the VNr derived from the RSM, with the VNr calculated based on the oPR, estimated by the $H_2O_2 \times HCHO/NO_2$ indicator and denoted as oVNr. Consistent spatial and temporal variations were found for VNr and oVNr. Additional simultaneous VOC control is required in January and in northern and eastern China, and is highly correlated with the low PR (Fig. 7). The domain-averaged oVNr values were estimated to be 0.95, 0.43, 0.38, and 0.47 in January, April, July, and October, respectively, with the highest and lowest oVNr values noted in January and July, respectively. That is comparable with VNr in the four study months (i.e., 0.82, 0.46, 0.34, and 0.57, respectively).

The annual-averaged VNr and PR were also calculated for each province in China (Fig. 11). VNr was negatively correlated with the PR at the provincial level. The northern provinces, namely Heilongjiang, Xinjiang, and Liaoning required the highest VNr (1-1.2) because their PRs were very low (0.3-0.4). In the NCP, including the province of Tianjin, Hebei, Henan, Shandong, Shanxi, Inner Mongolia, and Beijing, high VNr (0.7-0.9) was required to overcome the stronger NO_x-saturated regime (PR = 0.4-0.6). The coastal provinces, namely Fujian, and Guangdong, and middle-eastern provinces, namely Jiangxi and Hunan, also demonstrated relatively high PRs (>0.7) and low VNr (<0.3).

Atmos. Chem. Phys. Discuss., https://doi.org/10.5194/acp-2019-183
Manuscript under review for journal Atmos. Chem. Phys.
Discussion started: 22 May 2019

Atmospheric Chemistry and Physics Discussions

3.3.2. $PM_{2.5}$

Using the responsive FR indicator or its observable oFR indicator can rapidly identify NH_3-rich or NH_3-poor conditions, and this information can aid policy-makers in estimating the additional $PM_{2.5}$ benefit associated with simultaneous control of NH_3 and NO_x emissions (ΔC_NH_3). As discussed in Section 2.2, ΔC_NH_3 can be calculated from the RSM using the first derivative of the $PM_{2.5}$ responsive function to NH_3. Therefore, ΔC_NH_3 must be strongly associated with the secondary inorganic aerosol (SNA) concentration, as suggested in Fig. S8, which demonstrates a strong correlation between SNA concentration and ΔC_NH_3. The linear regression with high R^2 (>0.71) implies that the ΔC_NH_3 can be approximately calculated based on the SNA concentration.

The ΔC_NH_3 estimated based on the SNA concentration ($o\Delta C\_NH_3$; based on the regression function in Fig. S8) was compared with that derived from the RSM (Fig. 12). The $o\Delta C\_NH_3$ typically captured the spatial and temporal variation of ΔC_NH_3, suggesting large benefits in January and October, particularly in eastern China and the Sichuan Basin. The domain-averaged ΔC_NH_3 values were approximately 0.31, 0.22, 0.16, and 0.38 μg m^{-3} $PM_{2.5}$ per 10 % NH_3 reduction in January, April, July, and October respectively. In April and July, $o\Delta C\_NH_3$ presented consistent results approximately 0.21 and 0.16 μg m^{-3} $PM_{2.5}$, respectively, per 10 % NH_3 reduction, but slightly underestimated the benefits in January and October (0.24 and 0.22 μg m^{-3} $PM_{2.5}$, respectively, per 10 % NH_3 reduction).

At the annual level, ΔC_NH_3 was compared with the population-weighted $PM_{2.5}$ concentration in each province (Fig. 13). ΔC_NH_3 ranged from 2 to 12 μg m^{-3} $PM_{2.5}$ per 10 % NH_3 reduction. In addition, the provinces with higher $PM_{2.5}$ exposure exhibited additional benefits from NH_3 reductions (i.e., high ΔC_NH_3), particularly in Hunan, Shandong, Tianjin, Jiangxi, Anhui, Henan, and Hubei where ΔC_NH_3 was > 8 μg m^{-3} $PM_{2.5}$ per 10 % NH_3 reduction. These benefits from simultaneous NH_3 control were substantial enough to be considered in these regions for achieving the national ambient $PM_{2.5}$ target (35

404 μg m^{-3}).

405 **3.3.3. Cobenefits of NO_x and VOC control in reducing O_3 and $PM_{2.5}$**

406 NO_x and VOCs are major precursors for O_3 and $PM_{2.5}$, and effectively controlling their emissions
407 can lead to cobenefits in reducing O_3 and $PM_{2.5}$. The PR results suggest strong NO_x-saturated regimes in
408 northern and eastern China and key regions, including the Sichuan Basin, YRD, and PRD, and
409 simultaneous VOC control is required to prevent increases in O_3 levels from the NO_x controls, based on a
410 certain VOC-to-NO_x ratio. $PM_{2.5}$ senstivity to NO_x can be negative under a strong NO_x-saturated regime;
411 this effect is not as significant as it is for O_3 (Fig. 3). We quantified the nonlinearity of $PM_{2.5}$ sensitivity to
412 NO_x by using the same PR concept but for $PM_{2.5}$ response (Text S2); Fig. S9 presents the spatial
413 distribution of the PR to identify $PM_{2.5}$ sensitivity to NO_x emission in the four study months. The PR
414 values for $PM_{2.5}$ were > 1 in April, July, and October in all grid cells across China, suggesting that NO_x
415 control is always beneficial for $PM_{2.5}$ reduction during these months. Even in January, the PR for $PM_{2.5}$
416 (0.4-0.8 in eastern and northern China) remains larger than that for O_3 (0.2-0.6 in eastern and northern
417 China), implying that the suggested VNr for O_3 was high enough to overcome the potential limitations on
418 $PM_{2.5}$ reduction from NO_x control.

419 To explore the cobenefits of reducing O_3 and $PM_{2.5}$ after simultaneous control of NO_x and VOCs,
420 we investigated the effectiveness of six control pathways with various VOC-to-NO_x ratios (Fig. 14). In
421 general, O_3 and $PM_{2.5}$ can be reduced in all months through simultaneous control of NO_x and VOCs. In
422 January (in the strong NO_x-saturated regime), $PM_{2.5}$ and O_3 requires simultaneous VOC control to prevent
423 the limitation of NO_x controls, whereas the required VNr is lower for $PM_{2.5}$ (approximately 0.4) than for
424 O_3 (approximately 0.8). The smaller VNr for $PM_{2.5}$ might be associated with the smaller PR for $PM_{2.5}$ as
425 well as the additional benefit of VOC controls in reducing secondary organic aerosols. In April and
426 October, simultaneous VOC controls were still required for O_3 (VNr = 0.2-0.6) but not for $PM_{2.5}$. In July

when NO_x-limited regime was dominant, the NO_x control was critical because the VOC controls had little effect on either O_3 or $PM_{2.5}$. At the annual level, the simultaneous VOC controls (40 % of the NO_x controls) led to cobenefits in reducing both O_3 and $PM_{2.5}$ at the national level. However, VNr varied significantly in different seasons, suggesting that considering the seasonality of O_3 and $PM_{2.5}$ chemistry is necessary for design of a season-specific control strategy.

4. Summary and conclusion

Compared with conducting multiple CTM simulations, the indicator method proved more efficient in identifying the chemical regime in the current scenarios. However, the traditional indicators are not as useful as the RSM-based PR and FR indicators for policy-makers to infer feasible emission reduction paths. Therefore, this study quantified the relationship between RSM-based and traditional-observable indicators and developed new observable response indicators, the oPR and oFR, which can be used to quantify the nonlinearity of O_3 and $PM_{2.5}$ response to precursor emissions. Similar to the traditional indicators, the oPR and oFR can be easily calculated using a combination of ambient concentrations of certain chemical species obtained from surface-monitored observations, modeling simulations, or even satellite retrievals. In addition, the observable responsive indicators can not only rapidly identify the chemical regime but also provide policy-makers with useful information, such as simultaneous VOC controls to prevent increases in O_3 levels from NO_x controls under the NO_x-saturated regime (i.e., VNr), as well as the additional benefit of simultaneously reducing NH_3 alongside NO_x control in $PM_{2.5}$ reductions (i.e., ΔC_NH_3).

This study proposed a new O_3-chemistry indicator, namely $H_2O_2 \times HCHO/NO_2$, and $PM_{2.5}$-chemistry indicator, namely the TAR, both of which exhibited the highest success rates among all the indicators. This study also suggested that the log-linear combinations of baseline H_2O_2, HCHO, and NO_2 concentrations could provide an approximate PR to quantify O_3 chemistry spatially and temporally.

Similarly, the log-linear combination of baseline concentrations of ammonia gas, nitric acid gas, particulate ammonium, sulfate and nitrate can be used to approximately estimate the FR for $PM_{2.5}$ chemistry. The VNr was highly correlated with the PR, suggesting that a stronger NO_x-saturated regime requires greater VOC control accompanied by NO_x control. The positive correlation between ΔC_NH_3 and the population-weighted $PM_{2.5}$ concentration suggested that a province with high $PM_{2.5}$ exposure can gain greater benefits from NH_3 reduction. Finally, simultaneous control of NO_x and VOC could reduce both O_3 and $PM_{2.5}$ throughout the year, and an effective control pathway (VNr = 0.4) could lead to the cobenefits of reducing both O_3 and $PM_{2.5}$. However, VNr varied significantly among the seasons and provinces, suggesting the necessity of considering the seasonality of chemistry and of designing a more localized control strategy for each province.

In conclusion, the two unique aspects of this study are as follows. First, quantification of the correlation of observable indicators with responsive indicators (Fig. 5 and 7) implied that the traditional observable indicators, based on monitored or satellite-retrieved concentrations, can be used to quantify the nonlinearity of $PM_{2.5}$ and O_3 to precursor emission and provide useful policy implications. Second, this study reported a promising method for efficiently establishing $PM_{2.5}$- and O_3- responsive functions to precursors for traditional responsive or reduced-form modeling studies. This study suggested that the PR or FR (a combination of coefficients in the polynomial functions in the pf-RSM) can be approximately estimated using the ambient concentration of certain chemical species. Similarly, all coefficients in polynomial functions can be calculated based on a set of ambient concentrations of certain chemical species. The simple log-linear regression method used in this study demonstrated the possibility that even in the presence of uncertainties in prediction, more advanced data analytics technologies such as deep learning may improve performance in future.

Data availability

The pf-RSM outputs and code package are available upon request from the corresponding author.

Author contribution

These authors contributed equally to this work: Jia Xing & Dian Ding. JX designed the methodology and wrote the paper. DD conducted the modeling experiment and analyzed the data. SW provided ideas and financial support and edited the paper. ZD and YZ helped with the modeling experiment. JK, CJ and JH provided ideas and edited the paper.

Acknowledgements

This work was supported in part by National Key R & D program of China (2017YFC0210006), National Research Program for Key Issues in Air Pollution Control (DQGG0301& DQGG0204), National Natural Science Foundation of China (21625701&51861135102), and Shanghai Environmental Protection Bureau (2016-12). This work was completed on the “Explorer 100” cluster system of Tsinghua National Laboratory for Information Science and Technology.

Disclaimer

Although this work was reviewed by EPA and approved for publication, the views in the article are those of the authors alone and do not necessarily reflect the policy of the Agency. Mention of commercial products does not constitute endorsement by the Agency.

Atmos. Chem. Phys. Discuss., https://doi.org/10.5194/acp-2019-183
Manuscript under review for journal Atmos. Chem. Phys.
Discussion started: 22 May 2019

Atmospheric Chemistry and Physics Discussions

Reference

Ansari, A. S., and S. N. Pandis: Response of inorganic PM to precursor concentrations, Environ. Sci. Technol., 32, 2706–2714, 1998.

Cohan, D.S., Hakami, A., Hu, Y., Russell, A.G.: Nonlinear response of ozone to emissions: source apportionment and sensitivity analysis. Environ. Sci. Technol., 39, 6739-6748, 2005.

Cohen, A.J., Brauer, M., Burnett, R., Anderson, H.R., Frostad, J., Estep, K., Balakrishnan, K., Brunekreef, B., Dandona, L., Dandona, R., Feigin, V.: Estimates and 25-year trends of the global burden of disease attributable to ambient air pollution: an analysis of data from the Global Burden of Diseases Study 2015. The Lancet, 389(10082), 1907-1918, 2017.

Dennis, R.L., Bhave, P.V. and Pinder, R.W. Observable indicators of the sensitivity of PM2. 5 nitrate to emission reductions—Part II: Sensitivity to errors in total ammonia and total nitrate of the CMAQ-predicted non-linear effect of SO2 emission reductions. Atmospheric Environment, 42(6), pp.1287-1300, 2008.

Ding, D., Xing, J., Wang, S. X., Liu, K. Y., and Hao, J. M.: Emission reductions dominate the decline of ambient PM2.5 concentration and related premature mortality during 2013-2017 in China, Environ. Health Perspect., (under review), 2019a.

Ding, D., Xing, J., Wang, S. X., and Hao, J. M.: Impacts of emissions and meteorological anomaly on China's ozone pollution in warm seasons during 2013-2017, Frontiers of Environmental Science & Engineering, (under review), 2019b.

Forouzanfar, M.H., Alexander, L., Anderson, H.R., Bachman, V.F., Biryukov, S., Brauer, M., Burnett, R., Casey, D., Coates, M.M., Cohen, A., Delwiche, K.: Global, regional, and national comparative risk assessment of 79 behavioural, environmental and occupational, and metabolic risks or clusters of risks in 188 countries, 1990–2013: a systematic analysis for the Global Burden of Disease Study 2013. The Lancet, 386 (10010), 2287–2323, 2015.

Freas, W. P., Martinez, E. L., Meyer, E. L., Possiel, N. C., and Sennett, D. H.: Procedures for quantifying relationships between photochemical oxidants and precursors: supporting documentation, 1978.

Friedlander, S.K. Smoke, dust and haze: Fundamentals of aerosol behavior. New York, Wiley-Interscience, 1977. 333pp.

Fuhrer, J., Val Martin, M. , Mills, G. , Heald, C.L., Harmens, H., Hayes, F., Sharps, K., Bender, J., Ashmore, M.R.: Current and future ozone risks to global terrestrial biodiversity and ecosystem processes. Ecology and evolution, 6(24), 8785-8799, 2016.

Gipson, G. L., Freas, W. P., Kelly, R. F., and Meyer, E. L.: Guideline for use of city-specific EKMA in preparing ozone SIPs. EPA-450/4-80-027, US Environmental Protection Agency, Research Triangle Park, North Carolina, USA, 1981.

Hakami, A., Odman, M.T., Russell, A.G.: Nonlinearity in atmospheric response: A direct sensitivity analysis approach. Journal of Geophysical Research: Atmospheres, 109(D15), 2004.

Hammer, M.U., Vogel, B. and Vogel, H.: Findings on H2O2/HNO3 as an indicator of ozone sensitivity in Baden-Württemberg, Berlin-Brandenburg, and the Po valley based on numerical simulations. Journal of Geophysical Research: Atmospheres, 107(D22), 2002.

Jiménez, P. and Baldasano, J.M.: Ozone response to precursor controls in very complex terrains: Use of photochemical indicators to assess O3-NOx-VOC sensitivity in the northeastern Iberian Peninsula. Journal of Geophysical Research: Atmospheres, 109(D20), 2004.

Jin, X., Fiore, A.M., Murray, L.T., Valin, L.C., Lamsal, L.N., Duncan, B., Folkert Boersma, K., De Smedt, I., Abad, G.G., Chance, K. and Tonnesen, G.S.: Evaluating a Space-Based Indicator of Surface

Ozone-NOx-VOC Sensitivity Over Midlatitude Source Regions and Application to Decadal Trends. Journal of Geophysical Research: Atmospheres, 122(19), 2017.

Li, K., Jacob, D.J., Liao, H., Shen, L., Zhang, Q. and Bates, K.H.: Anthropogenic drivers of 2013–2017 trends in summer surface ozone in China. *Proceedings of the National Academy of Sciences*, *116*(2), pp.422-427, 2019.

Liang, J., Jackson, B. and Kaduwela, A.: Evaluation of the ability of indicator species ratios to determine the sensitivity of ozone to reductions in emissions of volatile organic compounds and oxides of nitrogen in northern California. Atmospheric Environment, 40(27), pp.5156-5166, 2006.

Liu, X.H., Zhang, Y., Xing, J., Zhang, Q., Wang, K., Streets, D.G., Jang, C., Wang, W.X., Hao, J.M.: Understanding of regional air pollution over China using CMAQ, part II. Process analysis and sensitivity of ozone and particulate matter to precursor emissions. Atmospheric Environment, 44(30), 3719-3727, 2010.

Lu, C.H. and Chang, J.S.: On the indicator-based approach to assess ozone sensitivities and emissions features. Journal of Geophysical Research: Atmospheres, 103(D3), pp.3453-3462, 1998.

Lu, X., Hong, J., Zhang, L., Cooper, O. R., Schultz, M. G., Xu, X., Wang, T., Gao, M., Zhao, Y., and Zhang, Y.: Severe Surface Ozone Pollution in China: A Global Perspective, Environmental Science & Technology Letters, 5, 487-494, 10.1021/acs.estlett.8b00366, 2018.

Megaritis, A.G., Fountoukis, C., Charalampidis, P.E., Pilinis, C. and Pandis, S.N.: Response of fine particulate matter concentrations to changes of emissions and temperature in Europe. Atmospheric Chemistry and Physics, 13(6), 3423-3443, 2013.

Milford, J. B., Gao, D. F., Sillman, S., Blossey, P., and Russell, A. G.: Total reactive nitraogen (NOy) as an indicator of the sensitivity of ozone to reductions in hydrocarbon and NOx emissions, Journal of Geophysical Research-Atmospheres, 99, 3533-3542, 10.1029/93jd03224, 1994.

Myhre, G., Shindell, D., Bréon, F.M., Collins, W., Fuglestvedt, J., Huang, J., Koch, D., Lamarque, J.F., Lee, D., Mendoza, B., Nakajima, T. Anthropogenic and Natural Radiative Forcing. In: Climate Change 2013: The Physical Science Basis. Contribution of Working Group I to the Fifth Assessment Report of the Intergovernmental Panel on Climate Change, T.F. Stocker et al, Eds. Cambridge Univ. Press, 2013, 659-740.

Oak Ridge National Laboratory. Landscan global population dataset 2012. Oak Ridge, Tennessee: Oak Ridge National Laboratory, 2013

Peng, Y.P., Chen, K.S., Lai, C.H., Lu, P.J. and Kao, J.H.: Concentrations of H2O2 and HNO3 and O3–VOC–NOx sensitivity in ambient air in southern Taiwan. Atmospheric Environment, 40(35), pp.6741-6751, 2006.

Pinder, R.W., Dennis, R.L. and Bhave, P.V.: Observable indicators of the sensitivity of PM2. 5 nitrate to emission reductions—Part I: Derivation of the adjusted gas ratio and applicability at regulatory-relevant time scales. Atmospheric Environment, 42(6), pp.1275-1286, 2008.

Pun, B.K., Seigneur, C., Bailey, E.M., Gautney, L.L., Douglas, S.G., Haney, J.L., Kumar, N.: Response of atmospheric particulate matter to changes in precursor emissions: a comparison of three air quality models. Environmental science & technology, 42(3), 831-837, 2007.

Seinfeld, J.H. and Pandis, S.N.: Atmospheric chemistry and physics: from air pollution to climate change. John Wiley & Sons, 2012.

Sillman, S.: The use of NO y, H2O2, and HNO3 as indicators for ozone-NO x-hydrocarbon sensitivity in urban locations. Journal of Geophysical Research: Atmospheres, 100(D7), pp.14175-14188., 1995.

Sillman, S., He, D., Cardelino, C. and Imhoff, R.E.: The use of photochemical indicators to evaluate ozone-NOx-hydrocarbon sensitivity: Case studies from Atlanta, New York, and Los Angeles. *Journal of the Air & Waste Management Association*, *47*(10), pp.1030-1040, 1997.

583 Sillman, S., and D. He, Some theoretical results concerning O3-NOx-VOC chemistry and NOx-VOC
584 indicators, J. Geophys. Res., 107(D22), 4659, doi:10.1029/2001JD001123, 2002.
585 Sun, Y., Liu, C., Palm, M., Vigouroux, C., Notholt, J., Hu, Q., Jones, N., Wang, W., Su, W., Zhang, W.,
586 Shan, C., Tian, Y., Xu, X., De Mazière, M., Zhou, M., and Liu, J.: Ozone seasonal evolution and
587 photochemical production regime in the polluted troposphere in eastern China derived from high-
588 resolution Fourier transform spectrometry (FTS) observations, Atmos. Chem. Phys., 18, 14569-
589 14583, https://doi.org/10.5194/acp-18-14569-2018, 2018.
590 Takahama, S., Wittig, A.E., Vayenas, D.V., Davidson, C.I. and Pandis, S.N.: Modeling the diurnal variation
591 of nitrate during the Pittsburgh Air Quality Study. Journal of Geophysical Research: Atmospheres,
592 109(D16), 2004.
593 Tonnesen, G.S. and Dennis, R.L.: Analysis of radical propagation efficiency to assess ozone sensitivity to
594 hydrocarbons and NO x: 2. Long-lived species as indicators of ozone concentration sensitivity.
595 Journal of Geophysical Research: Atmospheres, 105(D7), pp.9227-9241, 2000.
596 Wang, J., Xing, J., Mathur, R., Pleim, J.E., Wang,, S., Hogrefe, C., Gan, C.M., Wong, D.C., Hao, J.:
597 Historical trends in PM2.5-related premature mortality during 1990–2010 across the northern
598 hemisphere. Environmental health perspectives, 125(3), 400pp, 2017.
599 Wang, S. X., Xing, J., Jang, C., Zhu, Y., Fu, J.S., Hao, J.: Impact assessment of ammonia emissions on
600 inorganic aerosols in east China using response surface modeling technique. Environ. Sci. Technol.,
601 45, 9293–9300, 2011.
602 Wang, S., Zhao, M., Xing, J., Wu, Y., Zhou, Y., Lei, Y., He, K., Fu, L., & Hao, J.: Quantifying the air
603 pollutants emission reduction during the 2008 Olympic Games in Beijing. Environmental science
604 & technology, 44(7), 2490-2496, 2010.
605 West, J.J., Ansari, A.S., Pandis, S.N. Marginal PM25: nonlinear aerosol mass response to sulfate
606 reductions in the Eastern United States. Journal of the Air & Waste Management Association,
607 49(12), 1415-1424, 1999.
608 Xing, J., Wang, S. X., Jang, C., Zhu, Y., and Hao, J. M.: Nonlinear response of ozone to precursor emission
609 changes in China: a modeling study using response surface methodology, Atmospheric Chemistry
610 and Physics, 11, 5027-5044, 10.5194/acp-11-5027-2011, 2011.
611 Xing, J., Ding, D., Wang, S., Zhao, B., Jang, C., Wu, W., Zhang, F., Zhu, Y., and Hao, J. Quantification of
612 the enhanced effectiveness of NOx control from simultaneous reductions of VOC and NH3 for
613 reducing air pollution in the Beijing–Tianjin–Hebei region, China, Atmos. Chem. Phys., 18, 7799-
614 7814, https://doi.org/10.5194/acp-18-7799-2018, 2018.
615 Xing, J., Wang, S., Zhao, B., Wu, W., Ding, D., Jang, C., Zhu, Y., Chang, X., Wang, J., Zhang, F. and Hao,
616 J.: Quantifying Nonlinear Multiregional Contributions to Ozone and Fine Particles Using an
617 Updated Response Surface Modeling Technique. Environmental science & technology,
618 51(20),11788-11798, 2017.
619 Ye, L., Wang, X., Fan, S., Chen, W., Chang, M., Zhou, S., Wu, Z. and Fan, Q.: Photochemical indicators
620 of ozone sensitivity: application in the Pearl River Delta, China. Frontiers of Environmental
621 Science & Engineering, 10(6), p.15, 2016.
622 Zhang, J., Wang, T., Chameides, W. L., Cardelino, C., Kwok, J., Blake, D. R., Ding, A., and So, K. L.:
623 Ozone production and hydrocarbon reactivity in Hong Kong, Southern China, Atmos. Chem. Phys.,
624 7, 557-573, https://doi.org/10.5194/acp-7-557-2007, 2007.
625 Zhang, Y., Wen, X. Y., Wang, K., Vijayaraghavan, K., and Jacobson, M. Z.: Probing into regional O-3 and
626 particulate matter pollution in the United States: 2. An examination of formation mechanisms
627 through a process analysis technique and sensitivity study, Journal of Geophysical Research-
628 Atmospheres, 114, 31, 10.1029/2009jd011900, 2009.

Zhao, B., Wang, S.X., Xing, J., Fu, K., Fu, J.S., Jang, C., Zhu, Y., Dong, X.Y., Gao, Y., Wu, W.J., Wang, J.D.: Assessing the nonlinear response of fine particles to precursor emissions: development and application of an extended response surface modeling technique v1.0. Geosci. Model Dev., 8, 115-128, 2015.

Zhao, B., Wu, W., Wang, S., Xing, J., Chang, X., Liou, K.N., Jiang, J.H., Gu, Y., Jang, C., Fu, J.S. and Zhu, Y.: A modeling study of the nonlinear response of fine particles to air pollutant emissions in the Beijing–Tianjin–Hebei region. Atmospheric Chemistry and Physics, 17(19), 12031-12050, 2017.

Zhao, B., Zheng, H., Wang, S., Smith, K.R., Lu, X., Aunan, K., Gu, Y., Wang, Y., Ding, D., Xing, J. and Fu, X. Change in household fuels dominates the decrease in PM2. 5 exposure and premature mortality in China in 2005–2015. Proceedings of the National Academy of Sciences, 115(49), pp.12401-12406, 2018.

Atmos. Chem. Phys. Discuss., https://doi.org/10.5194/acp-2019-183
Manuscript under review for journal Atmos. Chem. Phys.
Discussion started: 22 May 2019

Atmospheric Chemistry and Physics Discussions

643

644 **Table 1.** Terms in the pf-RSM design for O_3 and $PM_{2.5}$

Term	O_3	$PM_{2.5}$
1	NO_x^5	VOC
2	NO_x^4	NH_3
3	NO_x^3	NH_3^2
4	NO_x^2	NH_3^3
5	NO_x	SO_2
6	VOC	VOC^2
7	VOC^2	NO_xVOC
8	VOC^3	NO_x^2VOC
9	NO_xVOC	NO_x^4VOC
10	NO_xVOC^3	NO_xNH_3
11	NO_x^5VOC	NO_x
12	NO_x^2VOC	NO_x^2
13	SO_2	NO_x^3
14	NH_3	NO_x^4

645

646

Atmos. Chem. Phys. Discuss., https://doi.org/10.5194/acp-2019-183
Manuscript under review for journal Atmos. Chem. Phys.
Discussion started: 22 May 2019

Atmospheric Chemistry and Physics Discussions

647

648 **Table 2.** Summary of observable indicators and their performances in predicting O_3 chemistry

Indicator		success rate at TV (%)						success rate at TV' (%)				
	TV*	Jan	Apr	Jul	Oct	ANN	TV'	Jan	Apr	Jul	Oct	ANN
H_2O_2/HNO_3	0.2	68.8	74.9	89.0	60.8	73.4	**0.3**	77.9	83.0	90.4	70.6	80.5
$H_2O_2/(O_3+NO_2)$	0.02	81.1	41.9	85.4	57.4	66.4	**0.005**	69.2	73.3	88.8	53.3	71.1
NO_y	5	38.9	47.8	87.8	40.9	53.8	-	-	-	-	-	-
O_3/NO_x	15	56.5	75.8	58.8	71.7	65.7	-	-	-	-	-	-
O_3/NO_y	7	60.7	65.8	23.3	68.2	54.5	-	-	-	-	-	-
O_3/NO_z	7	43.5	75.0	76.4	67.0	65.5	-	-	-	-	-	-
$HCHO/NO_y$	0.28	83.9	32.5	19.4	50.9	46.7	**0.1**	66.7	77.7	86.3	75.6	76.6
$HCHO/NO_2$	1	87.3	49.7	27.4	73.8	59.6	**0.5**	75.7	77.2	69.1	82.2	76.1
$H_2O_2 \times HCHO/NO_2$	-	-	-	-	-	-	**0.3**	92.3	81.6	89.5	86.0	87.3

649 * TV- transition value as summaried in Zhang et al (2009); TV' - transition value proposed in this study

650

651

Atmos. Chem. Phys. Discuss., https://doi.org/10.5194/acp-2019-183
Manuscript under review for journal Atmos. Chem. Phys.
Discussion started: 22 May 2019

Atmospheric Chemistry and Physics Discussions

652

653 **Table 3.** Summary of observable indicators and their performances in predicting $PM_{2.5}$ chemistry

Indicator		success rate (%)				
	TV	Jan	Apr	Jul	Oct	ANN
Gas ratio (GR)	1*	51.7	59.3	69.6	41.7	55.6
Adjusted Gas ratio (AdjGR)	1*	81.8	73.3	74.0	67.5	74.1
Total Ammonia Ratio (TAR)	10**	86.2	77.5	80.6	74.0	79.6

654 * TV- transition value as proposed in Zhang et al (2009);

655 ** TV- transition value as proposed in this study

656

Atmos. Chem. Phys. Discuss., https://doi.org/10.5194/acp-2019-183
Manuscript under review for journal Atmos. Chem. Phys.
Discussion started: 22 May 2019

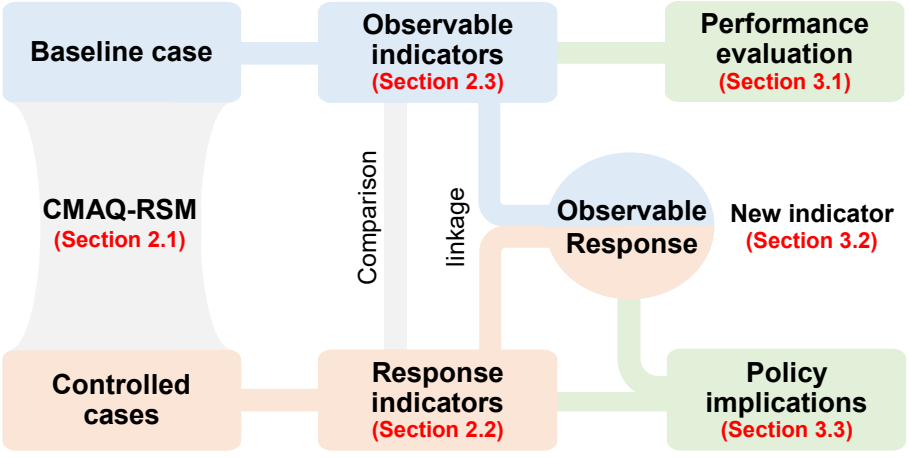

Figure 1. Flow of observable response indicator development and application

Atmos. Chem. Phys. Discuss., https://doi.org/10.5194/acp-2019-183
Manuscript under review for journal Atmos. Chem. Phys.
Discussion started: 22 May 2019

Atmospheric Chemistry and Physics Discussions

660

661

662 **Figure 2.** Simulation domain over mainland China (27 × 27-km^2 resolution, 182 × 232 grid cells). The
663 31 provinces are BJ-Beijing; TJ-Tianjin; HEB- Hebei; SX-Shanxi; IM-Inner Mongolia; LN- Liaoning;
664 JL- Jilin; HLJ-Helongjiang; SH- Shanghai; JS-Jiangsu; ZJ-Zhejiang; AH- Anhui; FJ- Fujian; JX-
665 Jiangxi; SD- Shandong; HEN- Henan; HUB-Hubei; HUN- Hunan; GD-Guangdong; GX- Guangxi; HN-
666 Hainan; CQ- Chongqing; SC- Sichuan; GZ-Guizhou; YN- Yunnan; TB- Tibet; SHX-Shaanxi; GS-
667 Gansu; QH-Qinghai; NX- Ningxia; and XJ-Xinjiang)

668

Atmos. Chem. Phys. Discuss., https://doi.org/10.5194/acp-2019-183
Manuscript under review for journal Atmos. Chem. Phys.
Discussion started: 22 May 2019

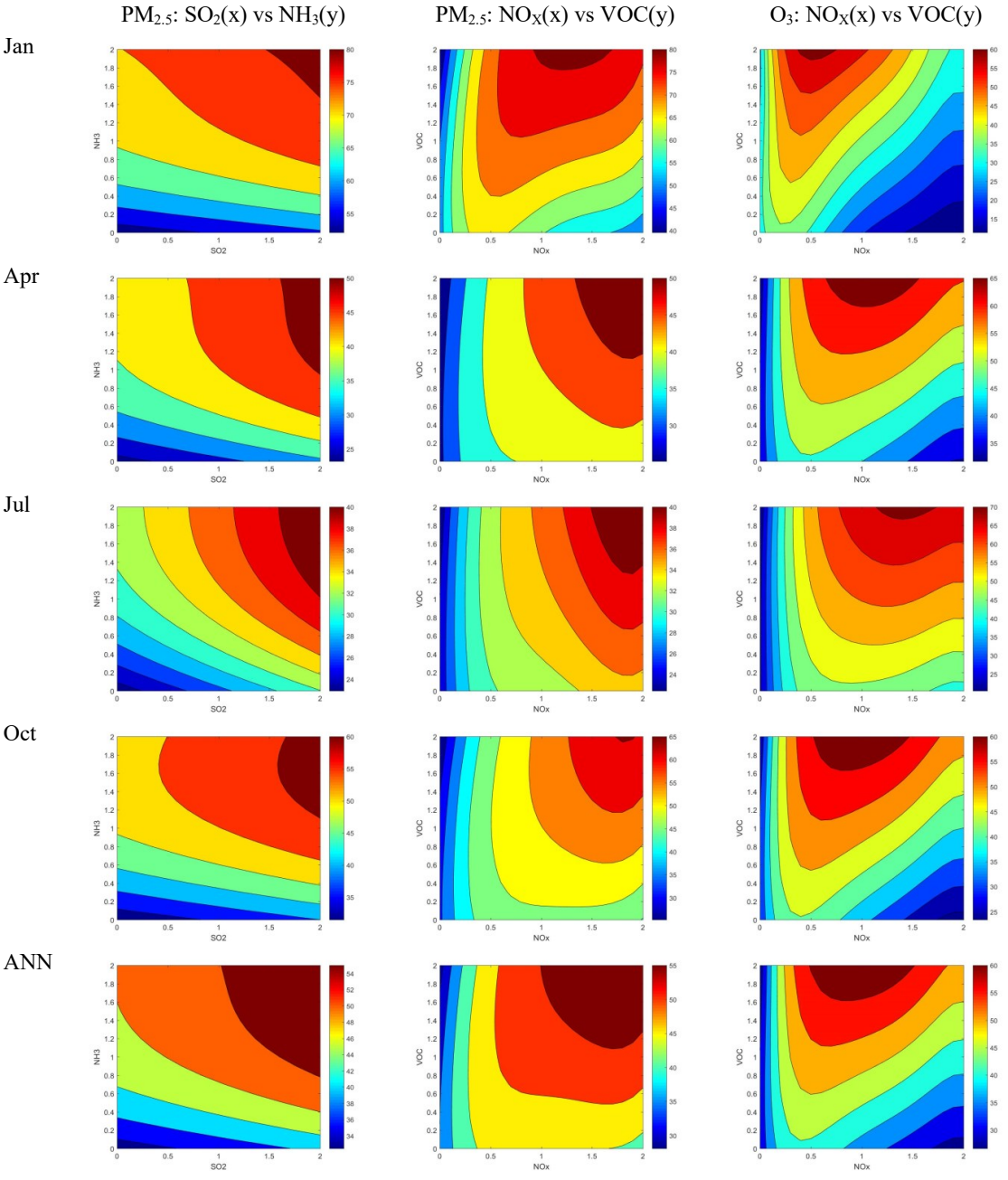

669 **Figure 3.** Isopleth of population-weighted $PM_{2.5}$ and daytime O_3 to precursor emission change in
670 different months. (The x-, y- axes represent precursor emission rates with a baseline of 1; background
671 colors represent the population-weighted $PM_{2.5}$ and daytime O_3 concentrations in China)

Atmos. Chem. Phys. Discuss., https://doi.org/10.5194/acp-2019-183
Manuscript under review for journal Atmos. Chem. Phys.
Discussion started: 22 May 2019

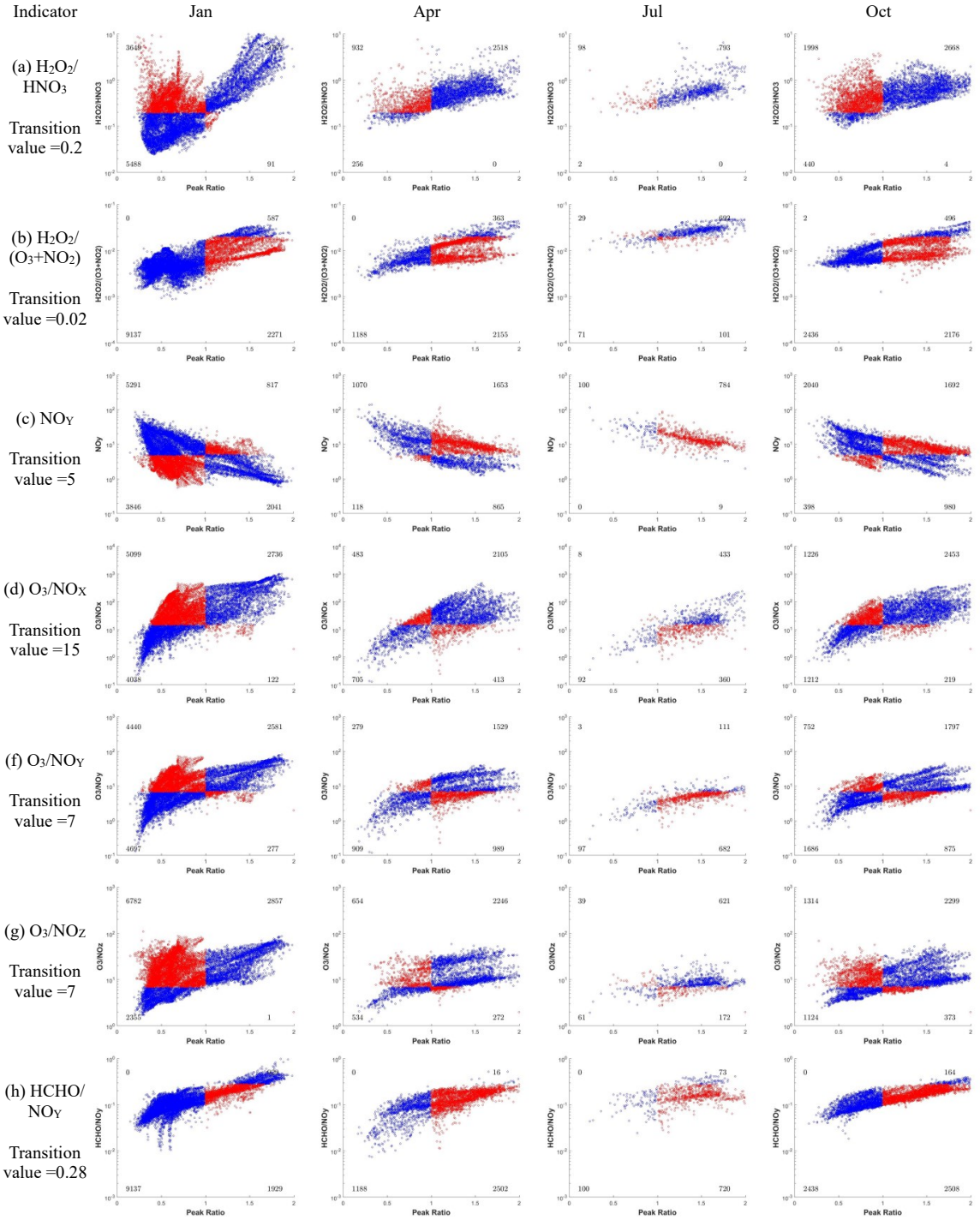

Atmos. Chem. Phys. Discuss., https://doi.org/10.5194/acp-2019-183
Manuscript under review for journal Atmos. Chem. Phys.
Discussion started: 22 May 2019

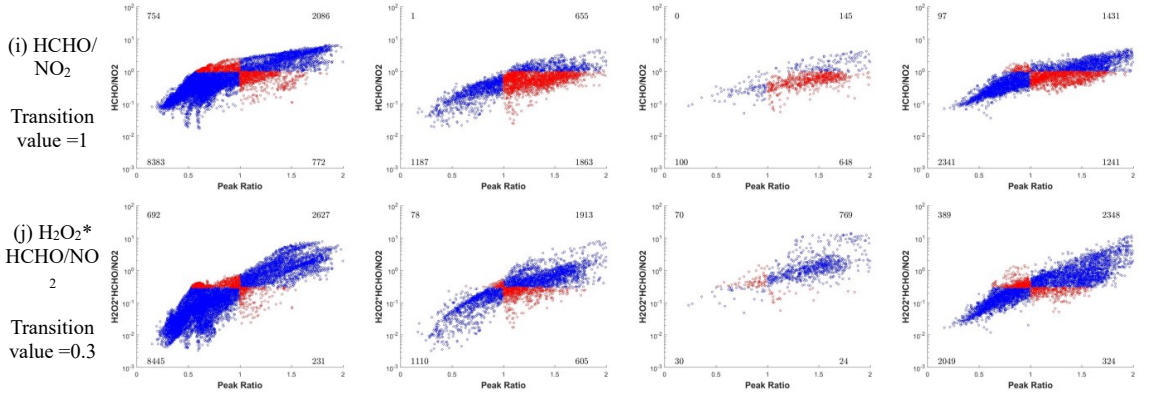

672 **Figure 4.** Performance of observable indicators in predicting O_3 chemistry. The x-axis represents the PR
673 values where the transition value is 1, and the y-axis represents the observable indicators. The blue dots
674 represent the grids where O_3 chemistry is successfully predicted by the observable indicator; the red dots
675 represent the grids where the observable indicator fails to predict O_3 chemistry. The numbers in the four
676 corners represent the grid number in each section; the number in July is much lower than those in the
677 other months because most grids are located at the NO_x-limited regime with PR > 2 in July.

678

Atmos. Chem. Phys. Discuss., https://doi.org/10.5194/acp-2019-183
Manuscript under review for journal Atmos. Chem. Phys.
Discussion started: 22 May 2019

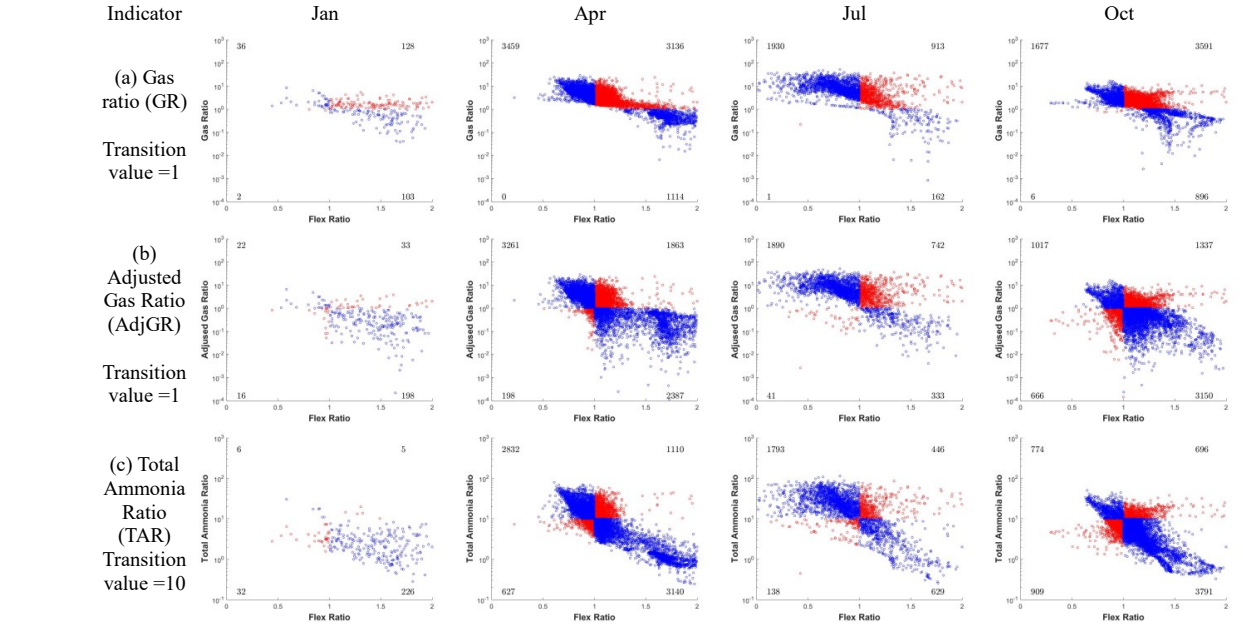

679 **Figure 5.** Performance of observable indicators in predicting $PM_{2.5}$ chemistry. The x-axis represents the
680 FR values where the transition value is 1, and the y-axis represents the observable indicators. The blue
681 dots represent the grids where $PM_{2.5}$ chemistry is successfully predicted by the observable indicator; the
682 red dots represent the grids where the observable indicator fails to predict $PM_{2.5}$ chemistry. The numbers
683 in the four corners represent the grid number in each section; the number in January is much lower than
684 those in the other months because most grids are located at the NH_3-poor condition with FR>2 in
685 January.

686

Atmos. Chem. Phys. Discuss., https://doi.org/10.5194/acp-2019-183
Manuscript under review for journal Atmos. Chem. Phys.
Discussion started: 22 May 2019

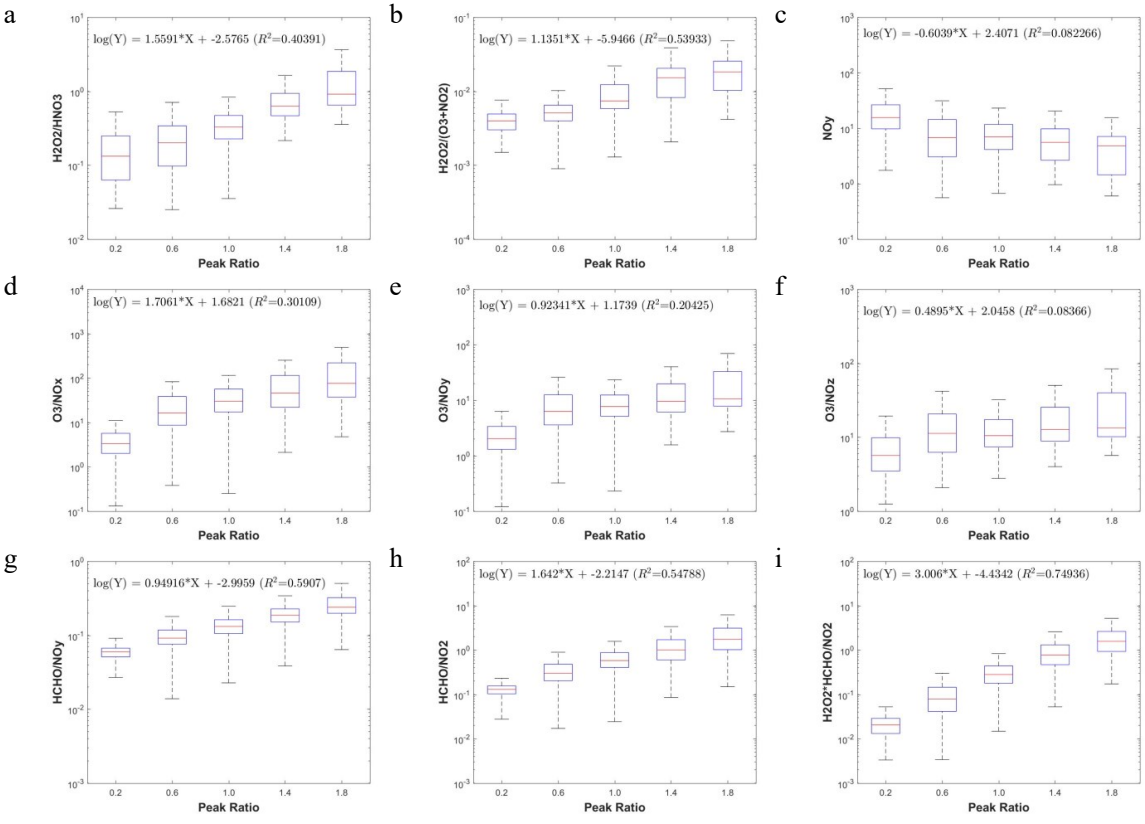

687 **Figure 6.** Development of observable responsive indicators for O_3 chemistry based on log-linear
688 regressions between observable indicators and the PR.

Atmos. Chem. Phys. Discuss., https://doi.org/10.5194/acp-2019-183
Manuscript under review for journal Atmos. Chem. Phys.
Discussion started: 22 May 2019

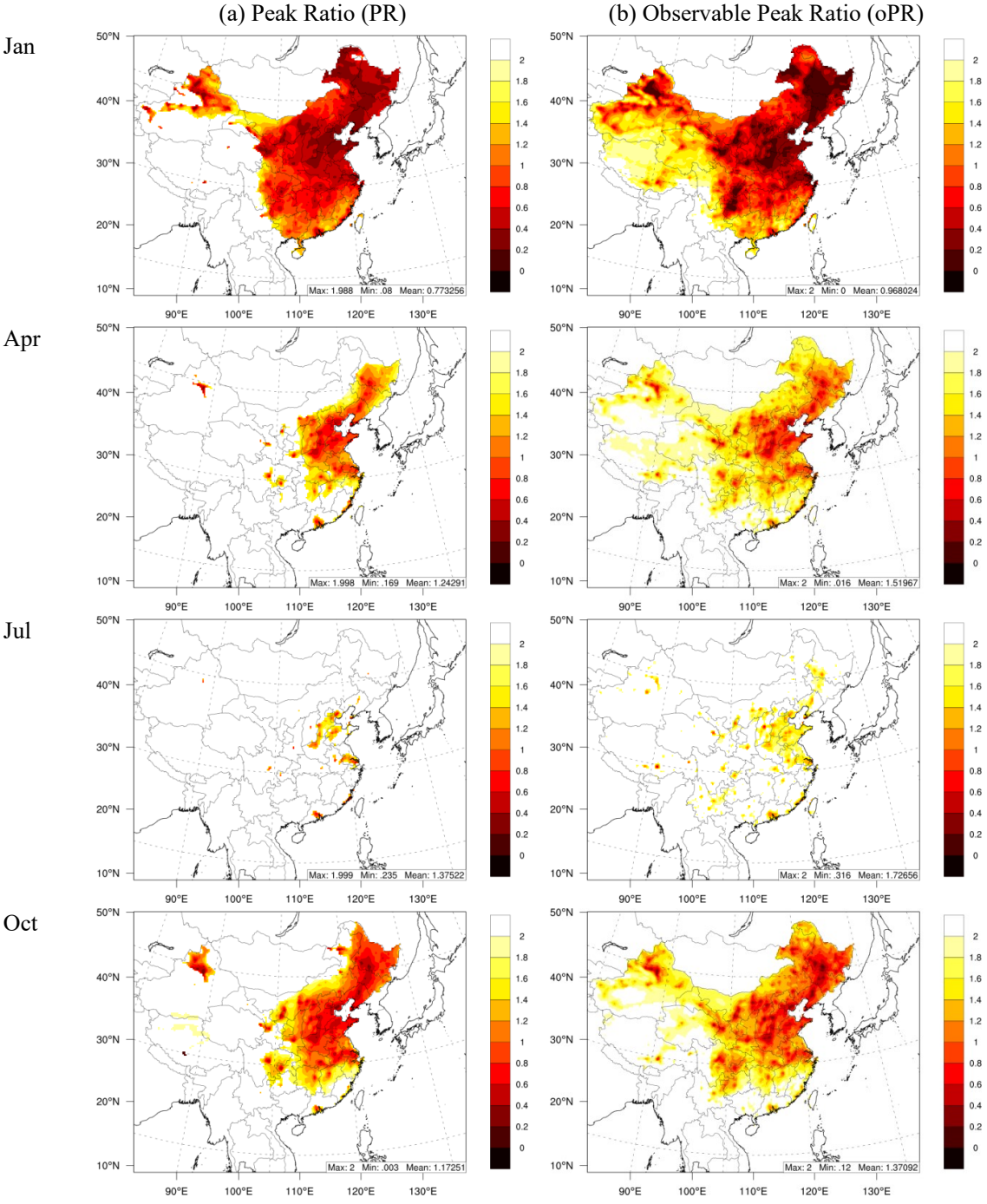

689 **Figure 7.** Comparison of the PR derived from the RSM with that calculated from concentrations for O_3
690 chemistry. The oPR was estimated based on $H_2O_2 \times HCHO/NO_2$.

Atmos. Chem. Phys. Discuss., https://doi.org/10.5194/acp-2019-183
Manuscript under review for journal Atmos. Chem. Phys.
Discussion started: 22 May 2019

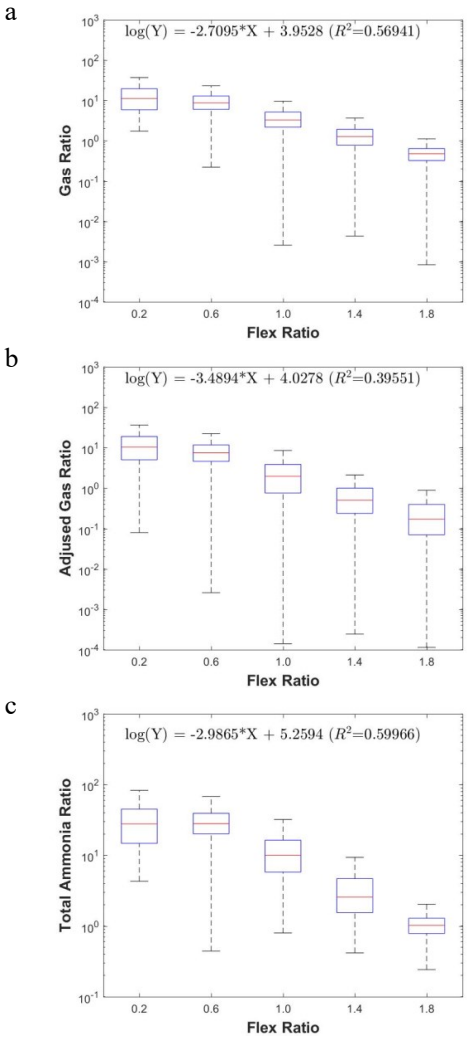

Figure 8. Development of observable responsive indicators for $PM_{2.5}$ chemistry based on log-linear regressions between observable indicators and the FR

Atmos. Chem. Phys. Discuss., https://doi.org/10.5194/acp-2019-183
Manuscript under review for journal Atmos. Chem. Phys.
Discussion started: 22 May 2019

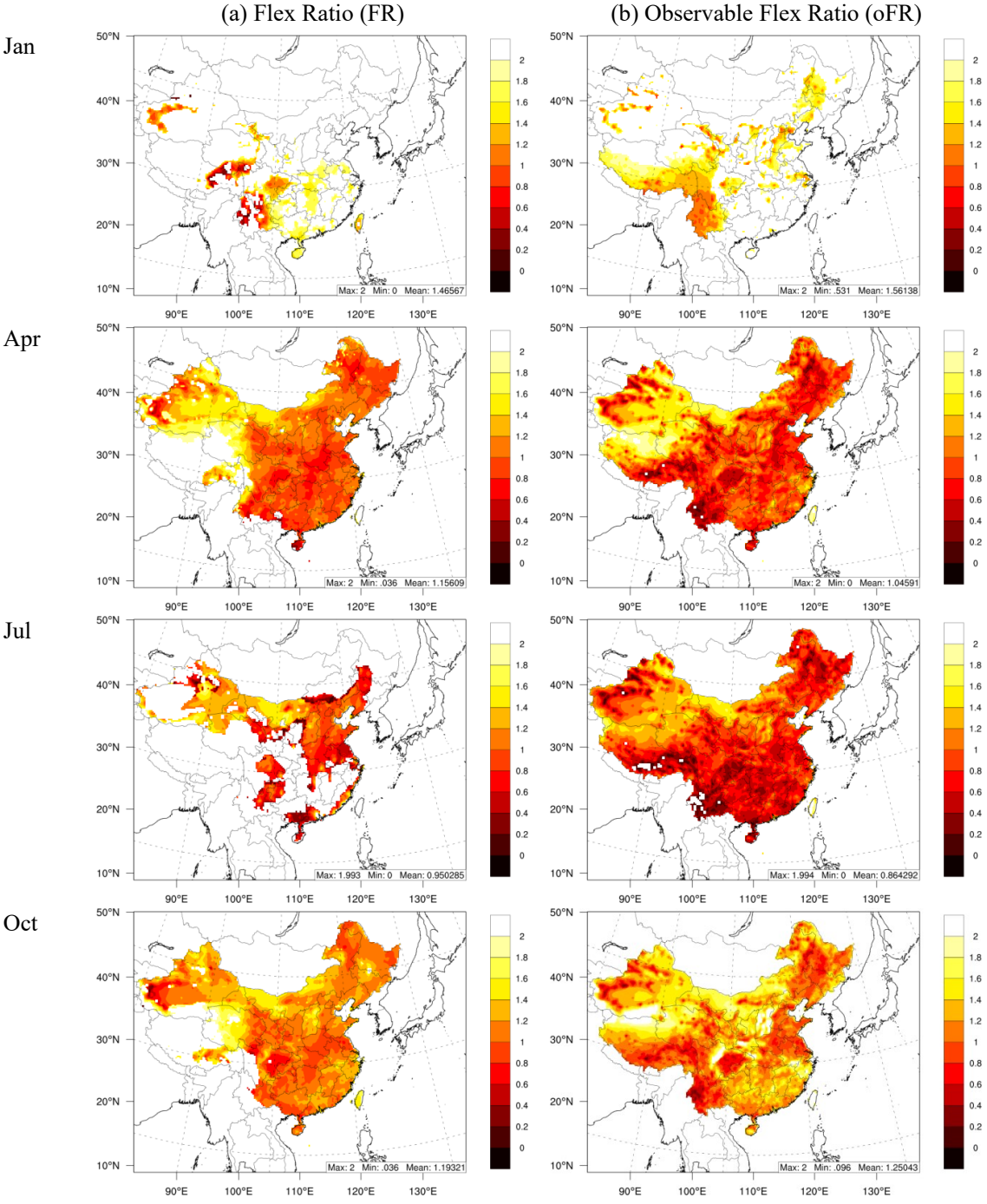

694 **Figure 9.** Comparison of the FR derived from the RSM with that calculated from concentrations for
695 $PM_{2.5}$ chemistry. The oPR was estimated based on TAR.

Atmos. Chem. Phys. Discuss., https://doi.org/10.5194/acp-2019-183
Manuscript under review for journal Atmos. Chem. Phys.
Discussion started: 22 May 2019

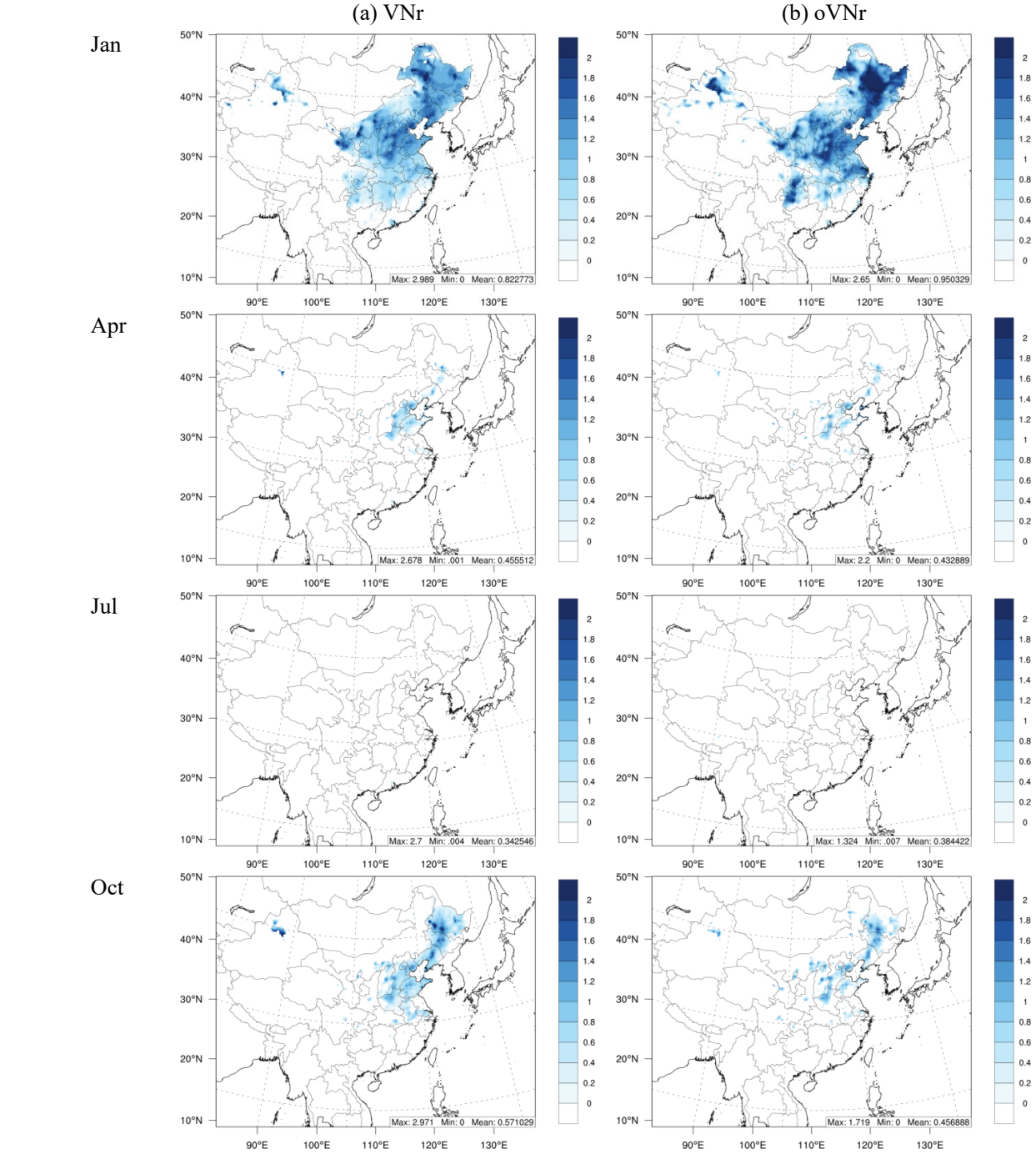

Figure 10. Comparison of VNr with oVNr.

Atmos. Chem. Phys. Discuss., https://doi.org/10.5194/acp-2019-183
Manuscript under review for journal Atmos. Chem. Phys.
Discussion started: 22 May 2019

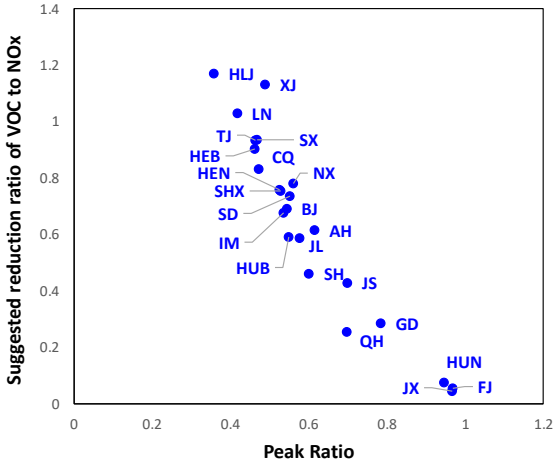

698

699 **Figure 11.** Comparison of the annual-averaged PR with VNr in each province in China

700

701

Atmos. Chem. Phys. Discuss., https://doi.org/10.5194/acp-2019-183
Manuscript under review for journal Atmos. Chem. Phys.
Discussion started: 22 May 2019

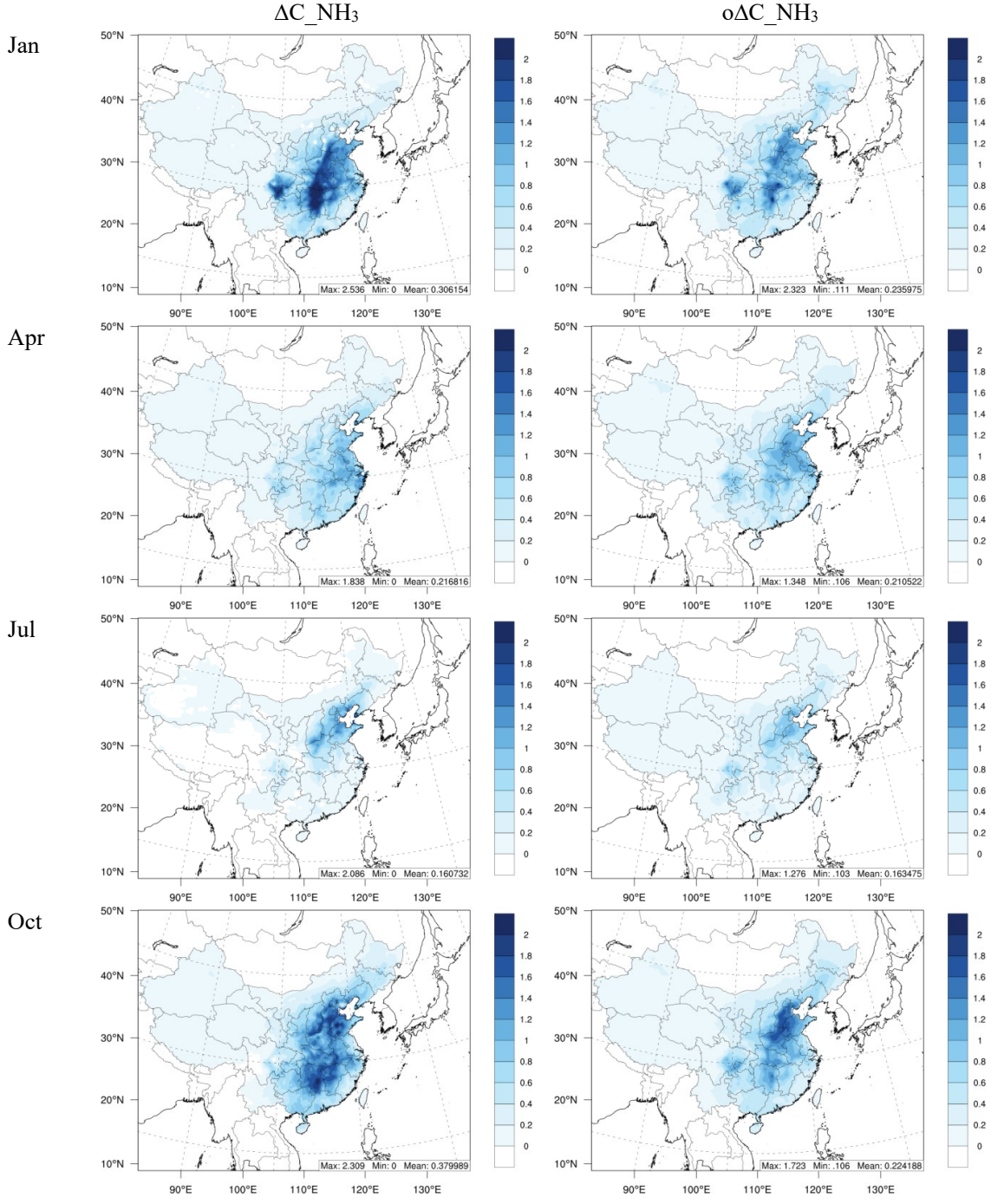

Figure 12. Comparion of the benefit in reducing $PM_{2.5}$ from simultaneous NH_3 reduction (ΔC_NH_3) with that calculated from concentrations ($o\Delta C\_NH_3$)

Atmos. Chem. Phys. Discuss., https://doi.org/10.5194/acp-2019-183
Manuscript under review for journal Atmos. Chem. Phys.
Discussion started: 22 May 2019

Atmospheric Chemistry and Physics Discussions

704

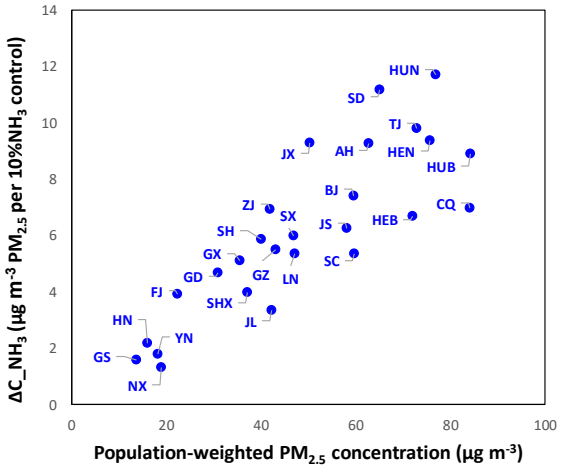

705

706 **Figure 13.** Comparison of annual-averaged benefit in reducing $PM_{2.5}$ from simultaneous NH_3 reduction
707 (ΔC_NH_3) and population-weighted $PM_{2.5}$ concentration in each province in China

708

Atmos. Chem. Phys. Discuss., https://doi.org/10.5194/acp-2019-183
Manuscript under review for journal Atmos. Chem. Phys.
Discussion started: 22 May 2019

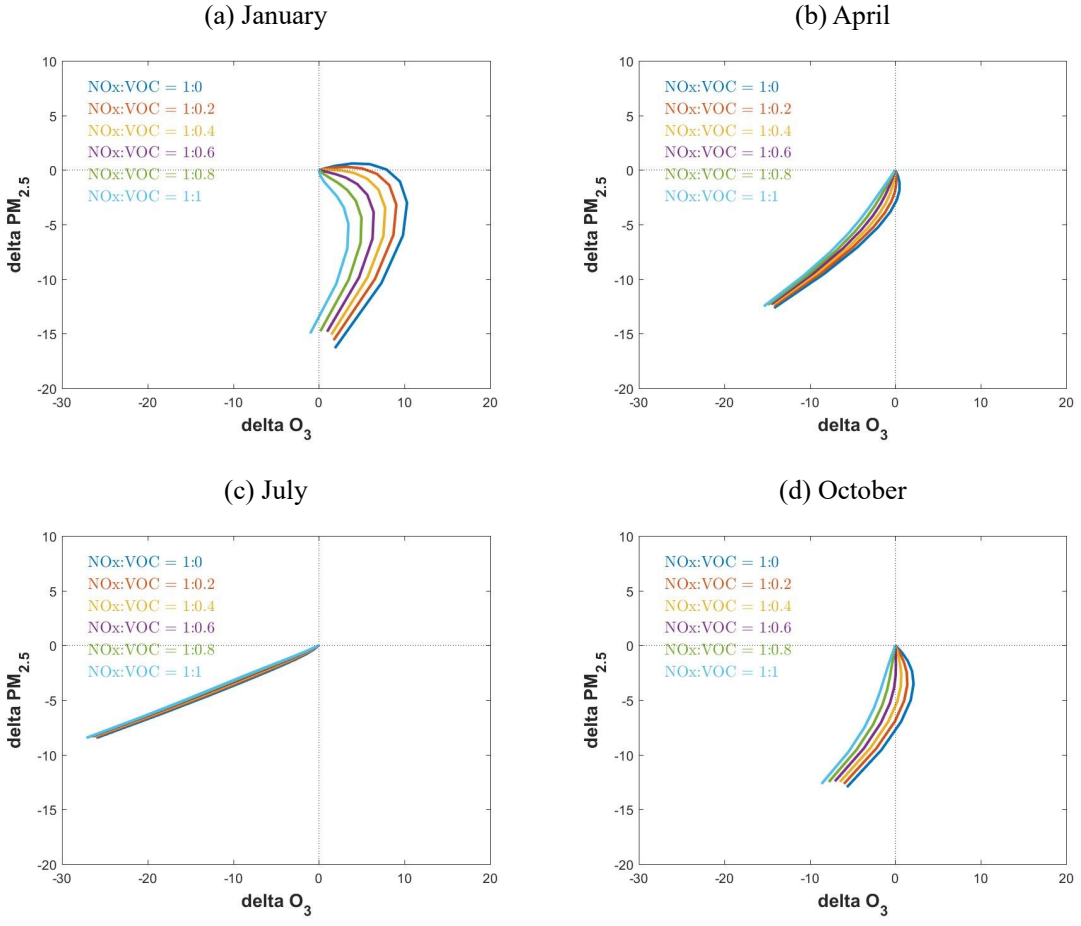

709 **Figure 14.** Control effectiveness with different NO_x and VOC ratios in reducing population-weighted
710 $PM_{2.5}$ and O_3 concentrations (in μg m^{-3}) in China (NO_x is from no control to 80 % reduction)